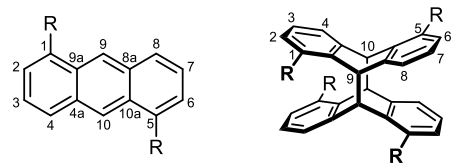


Electronic Supplementary Material (ESI)

Table of contents

NMR Spectroscopic Data	S2
Crystallographic Data	S20
References	S31

NMR Spectroscopic Data



Scheme 1: Numbering scheme for NMR spectroscopic assignments.

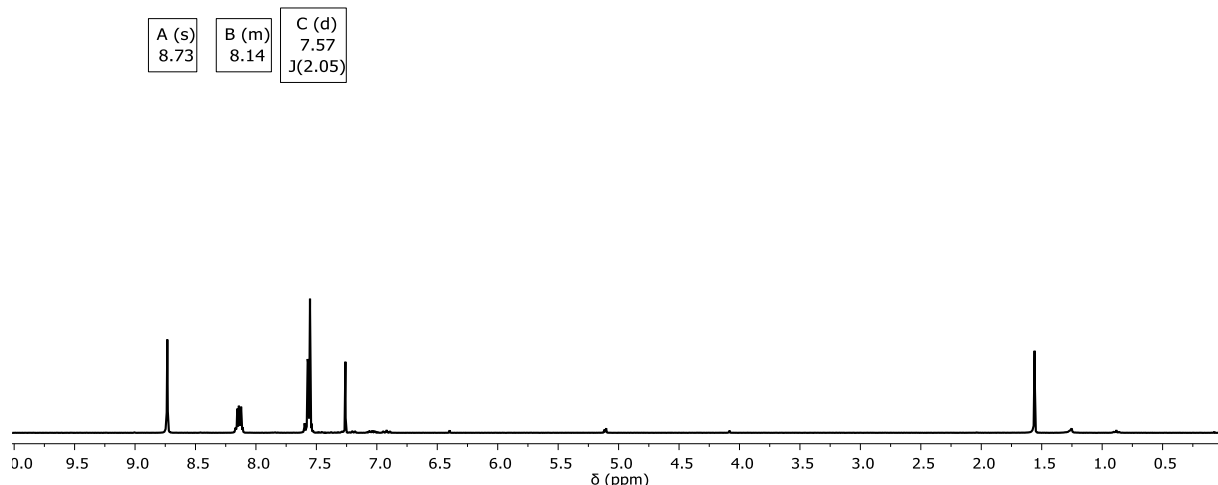


Figure S1: ^1H NMR spectrum of a solution of anthracene-1,5-diyl bis(trifluoromethanesulfonate) in CDCl_3 (293 K, 500 MHz).

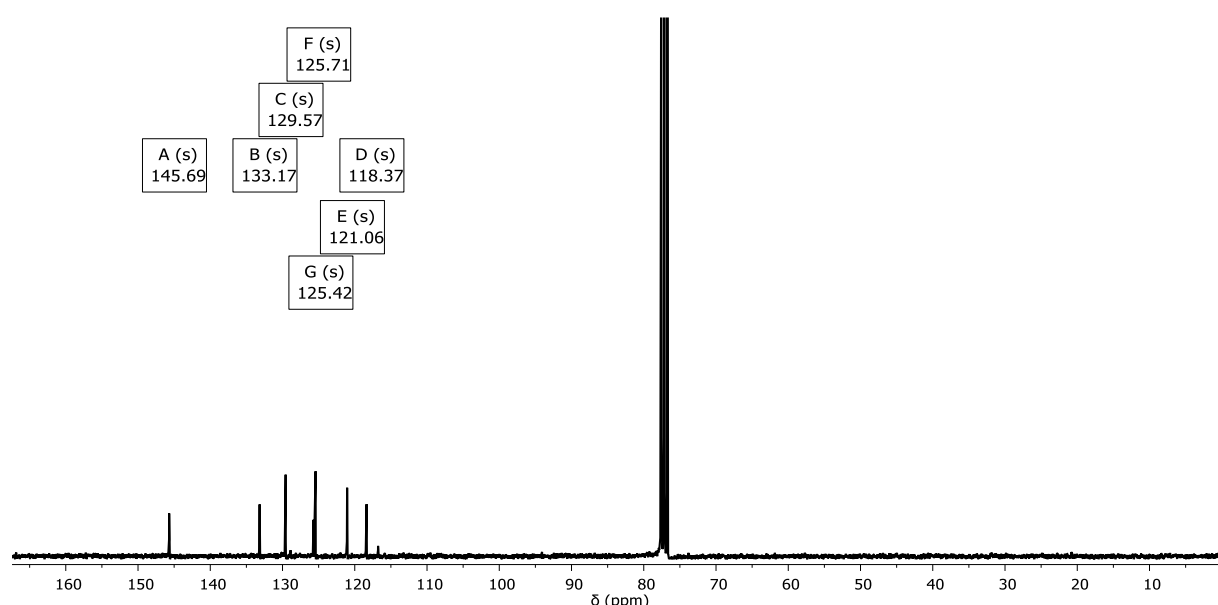


Figure S2: $^{13}\text{C}\{^1\text{H}\}$ NMR spectrum of a solution of anthracene-1,5-diyl bis(trifluoromethanesulfonate) in CDCl_3 (293 K, 75 MHz).

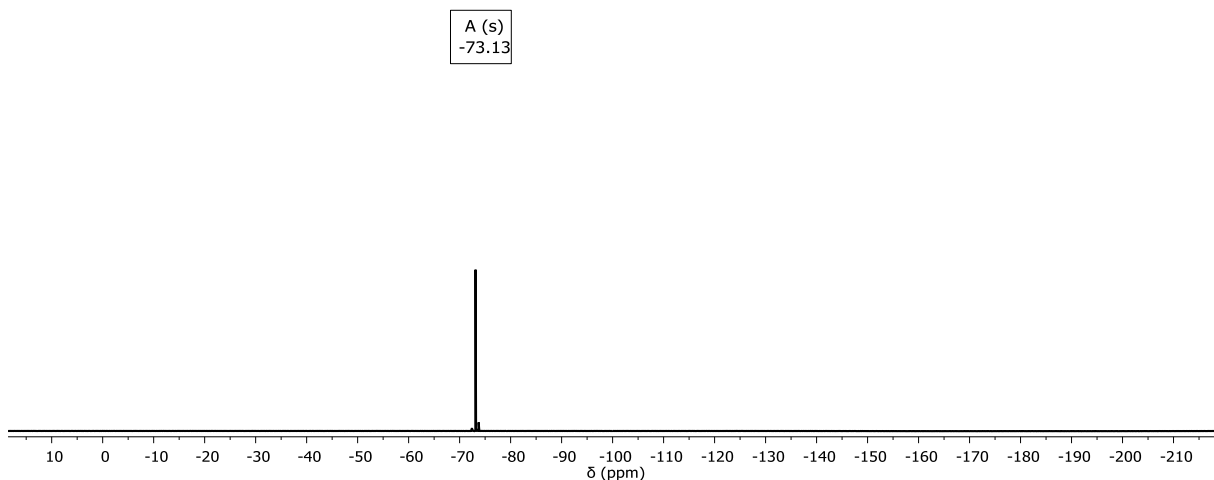


Figure S3: ¹⁹F NMR spectrum of a solution of anthracene-1,5-diyl bis(trifluoromethanesulfonate) in CDCl₃ (293 K, 282 MHz).

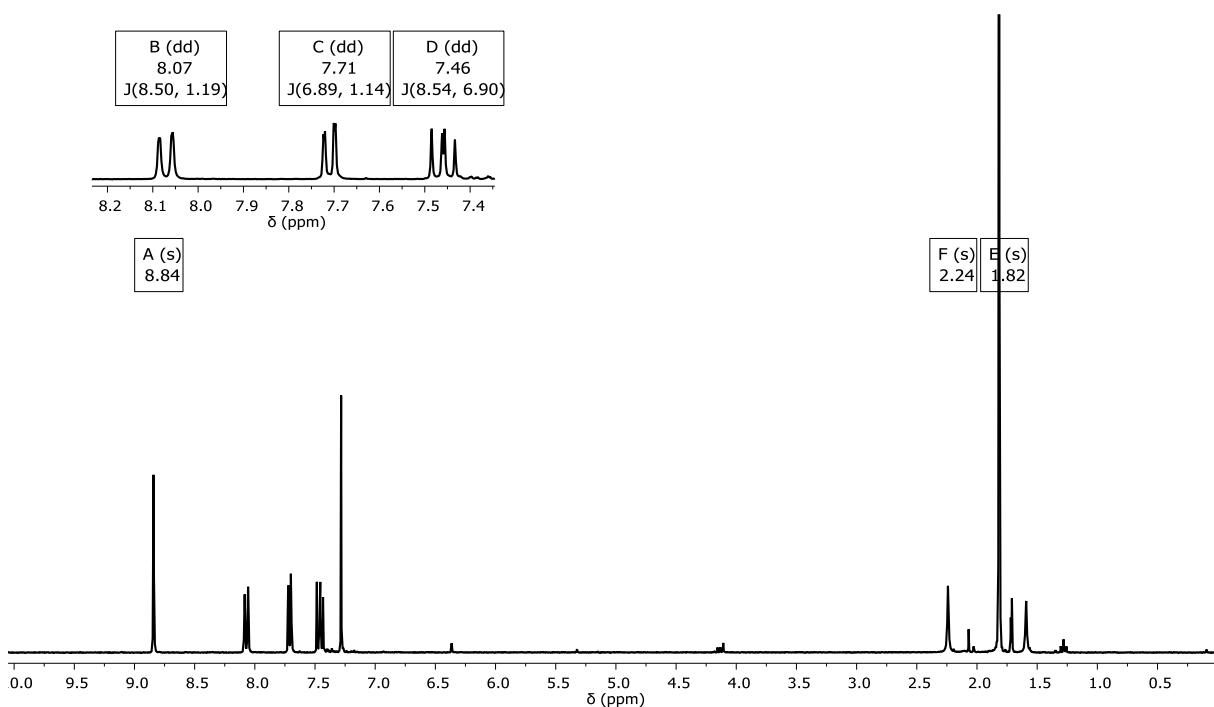


Figure S4: ¹H NMR spectrum of a solution of 1,5-di(3-methyl-3-hydroxy-1-butynyl)anthracene **3** in CDCl₃ (293 K, 282 MHz).

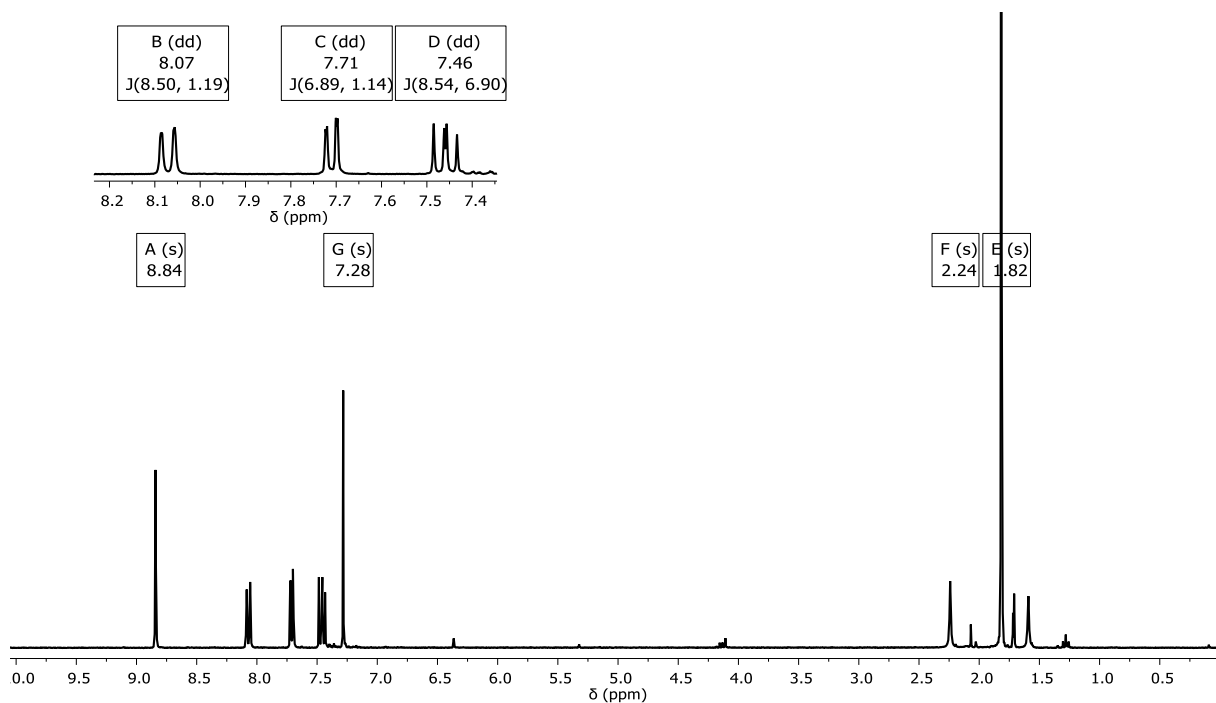


Figure S5: $^{13}\text{C}\{\text{H}\}$ NMR spectrum of a solution of 1,5-di(3-methyl-3-hydroxy-1-butynyl)anthracene **3** in CDCl_3 (293 K, 75 MHz).

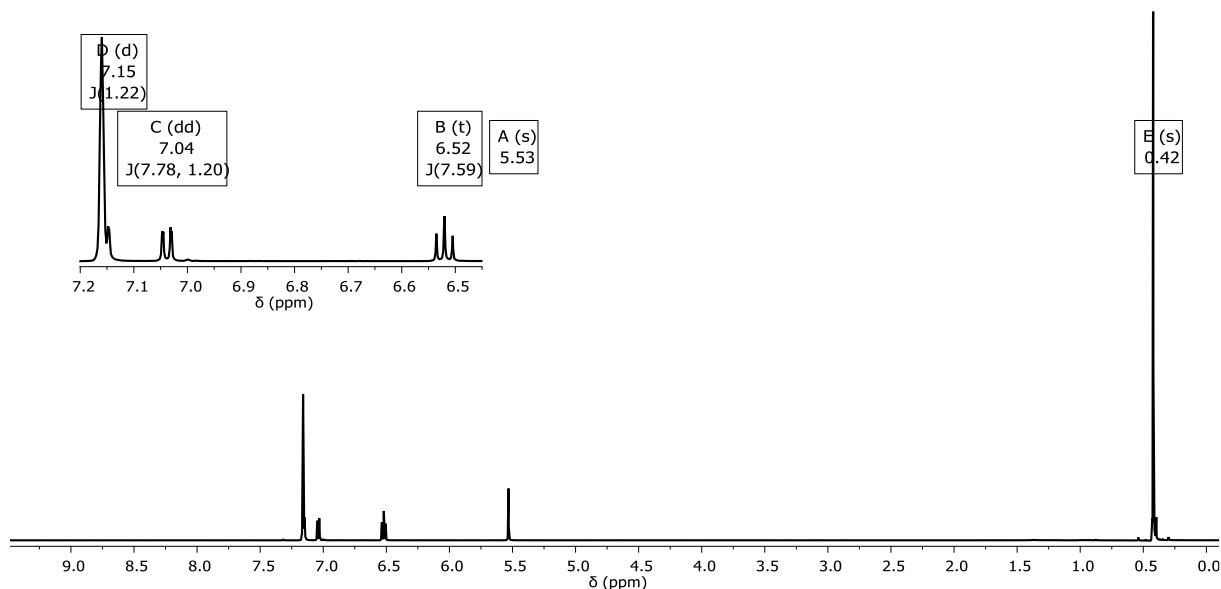


Figure S6: ^1H NMR spectrum of a solution of the photo-dimer of 1,5-bis(trimethylsilyl)ethynylanthracene (*anti*-**4**) in C_6D_6 (293 K, 500 MHz).

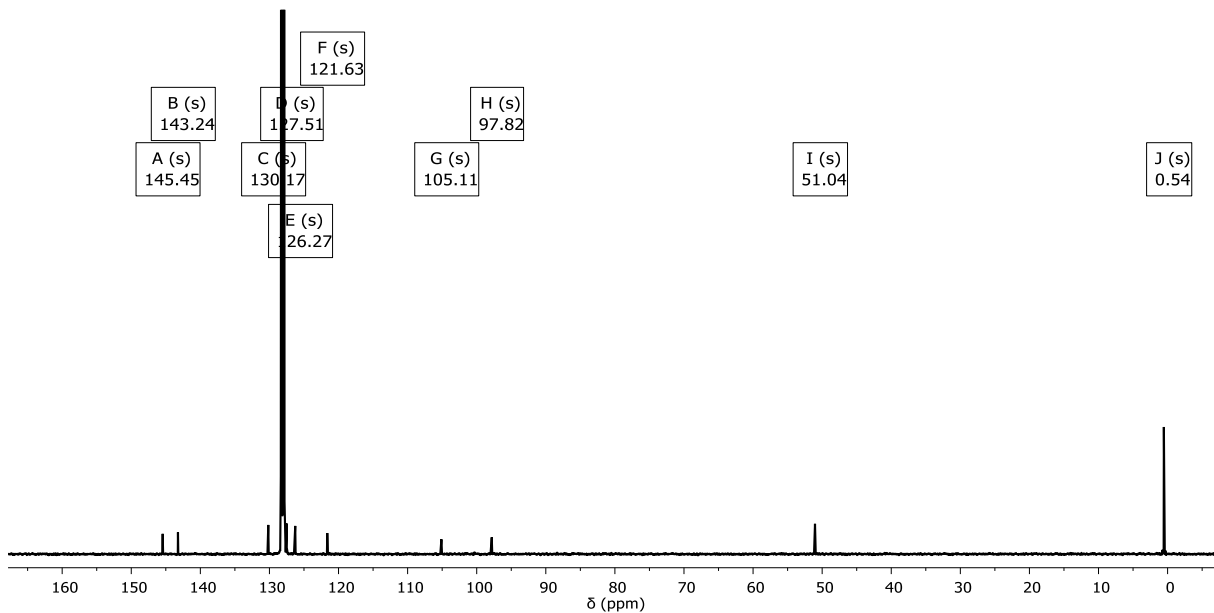


Figure S7: $^{13}\text{C}\{{}^1\text{H}\}$ NMR spectra of a solution of the photo-dimer of 1,5-bis((trimethylsilyl)ethynyl)anthracene (*anti*-**4**) in C_6D_6 (293 K, 126 MHz).

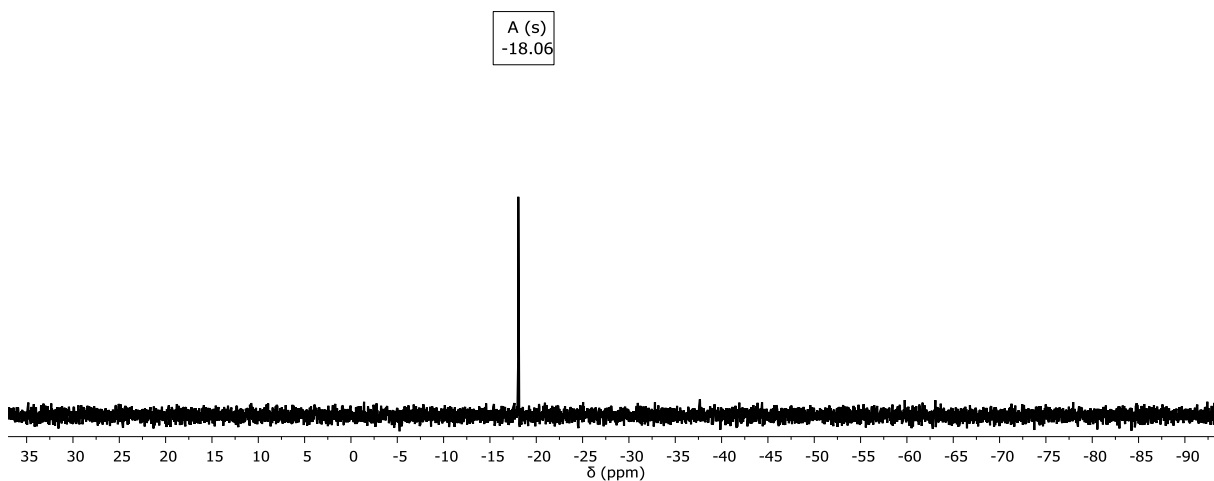


Figure S8: $^{29}\text{Si}\{{}^1\text{H}\}$ NMR spectrum of a solution of the *anti*-photo-dimer of 1,5-bis((trimethylsilyl)ethynyl)anthracene (*anti*-**4**) in C_6D_6 (293 K, 99 MHz).

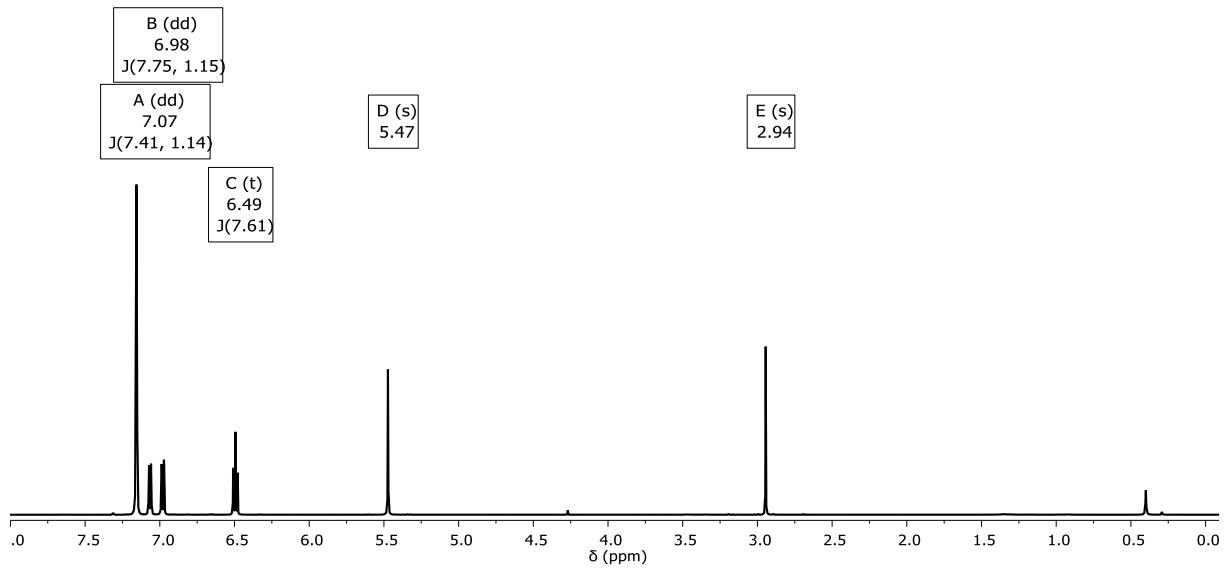


Figure S9: ^1H NMR spectrum of a solution of the *anti*-photo-dimer of 1,5-diethynylanthracene *anti*-5 in C_6D_6 (297 K, 500 MHz).

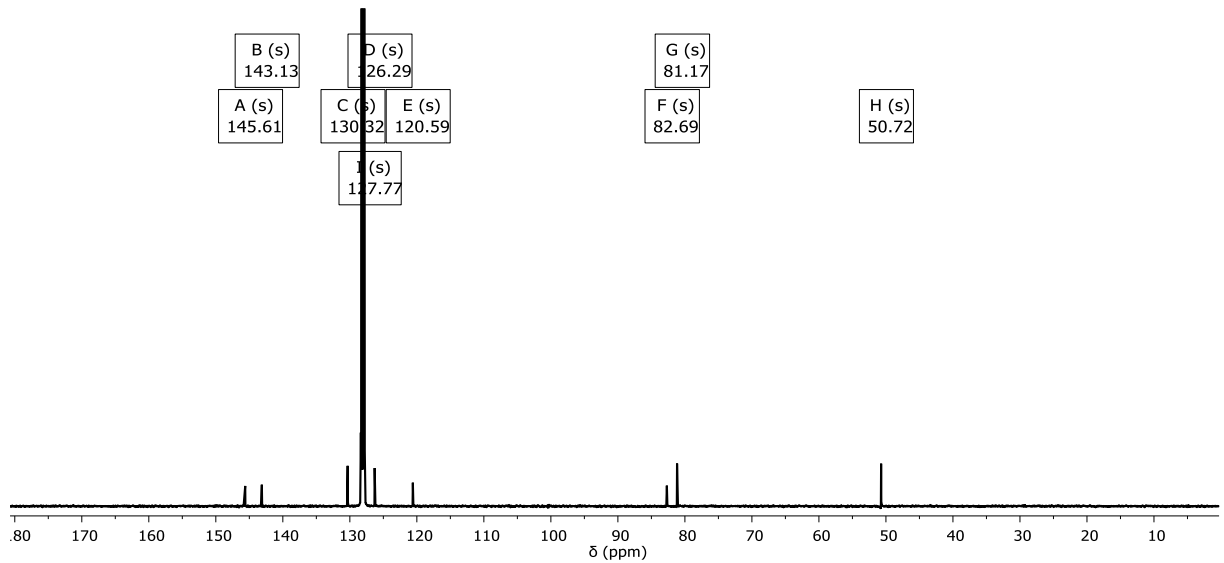


Figure S10: $^{13}\text{C}\{^1\text{H}\}$ NMR spectrum of a solution of the *anti*-photo-dimer of 1,5-diethynylanthracene *anti*-5 in C_6D_6 (297 K, 126 MHz).

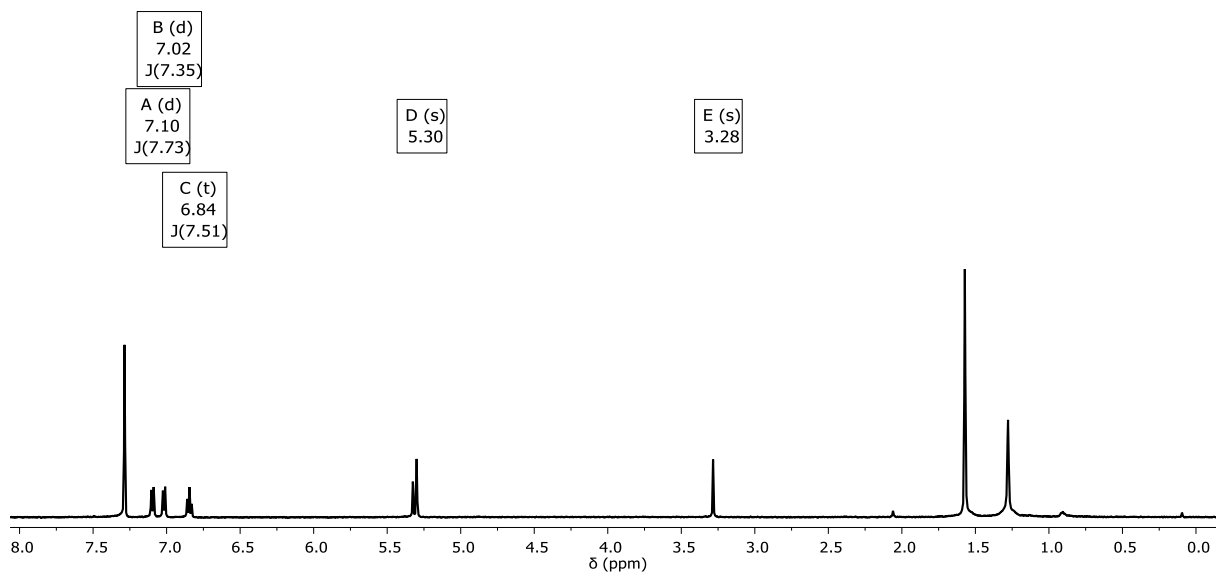


Figure S11: ^1H NMR spectrum of a solution of the *syn*-photo-dimer of 1,5-diethynylanthracene *syn*-5 in C_6D_6 (297 K, 500 MHz).

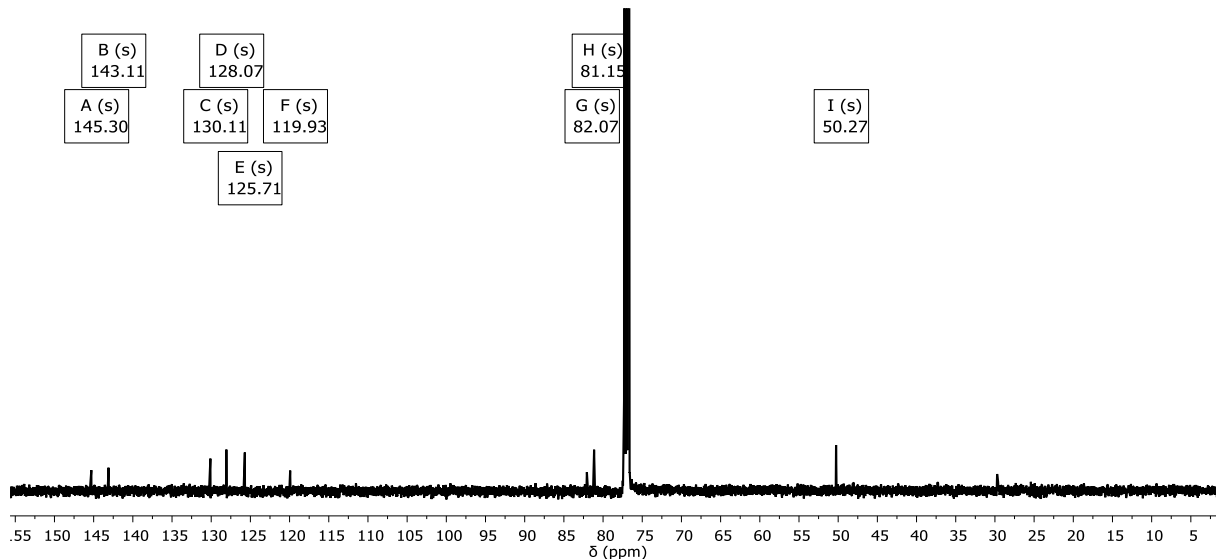


Figure S12: $^{13}\text{C}\{^1\text{H}\}$ NMR spectrum of a solution of the *anti*-photo-dimer of 1,5-diethynylanthracene *anti*-5 in C_6D_6 (297 K, 126 MHz).

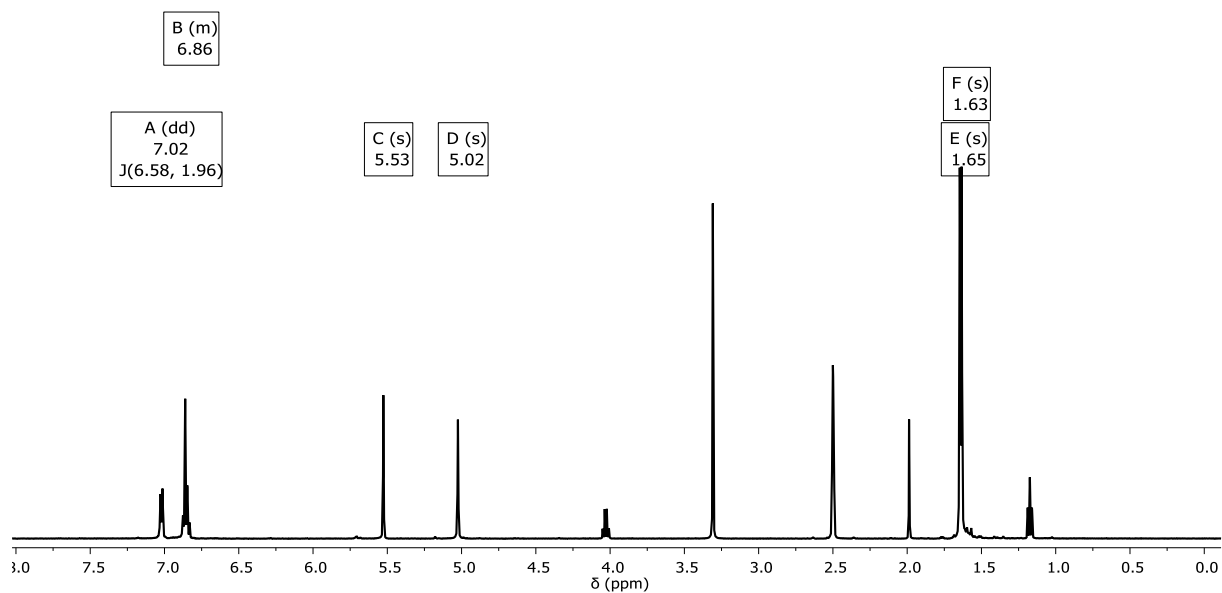


Figure S11: ^1H NMR spectrum of a solution of the *anti*-photo-dimer of **3 anti-6** in DMSO-d_6 (301 K, 500 MHz).

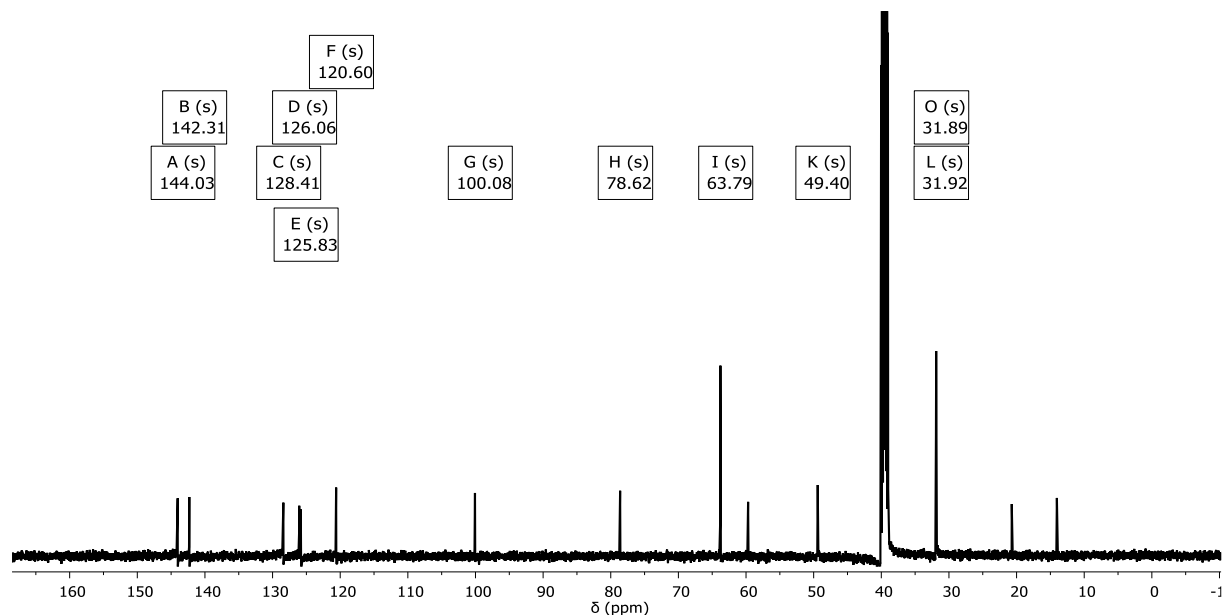


Figure S12: $^{13}\text{C}\{^1\text{H}\}$ spectrum of a solution of the *anti*-photo-dimer of **3 anti-6** in DMSO-d_6 (303 K, 126 MHz).

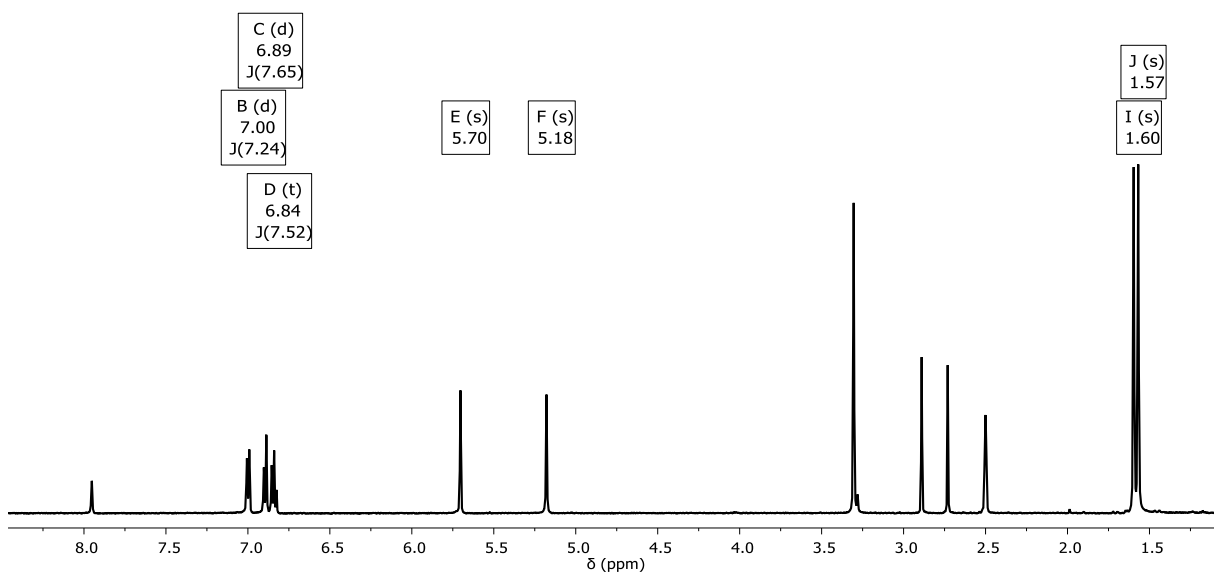


Figure S13: ^1H NMR spectrum of a solution of the *syn*-photo-dimer of **3** *syn*-**6** in DMSO-d_6 (301 K, 500 MHz).

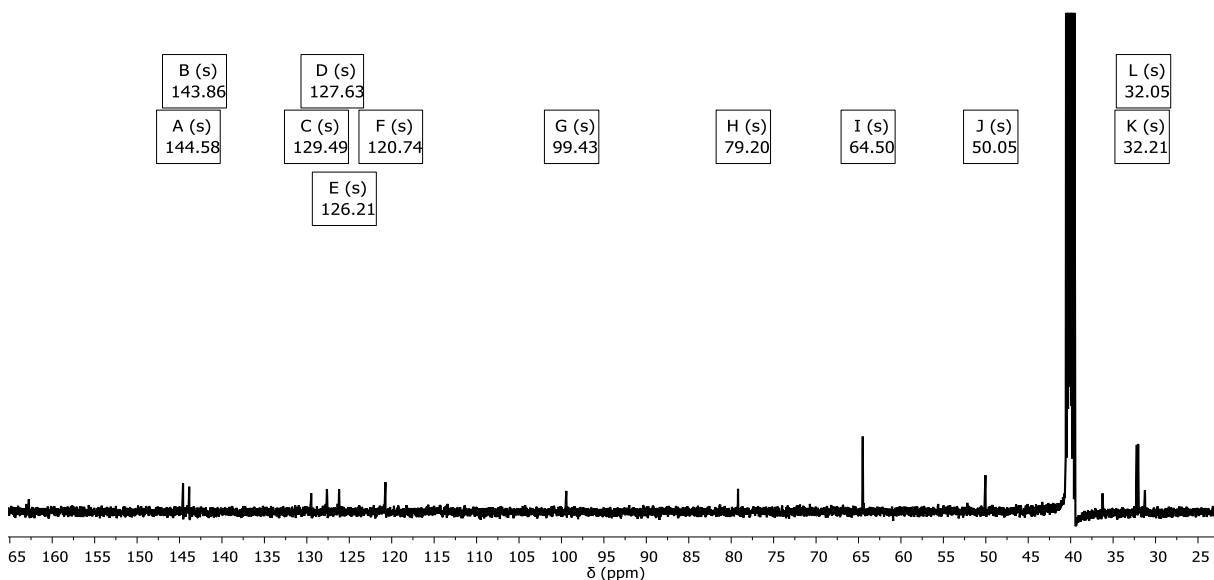


Figure S14: $^{13}\text{C}\{^1\text{H}\}$ spectrum of a solution of the *syn*-photo-dimer of **3** *syn*-**6** in DMSO-d_6 (303 K, 126 MHz).

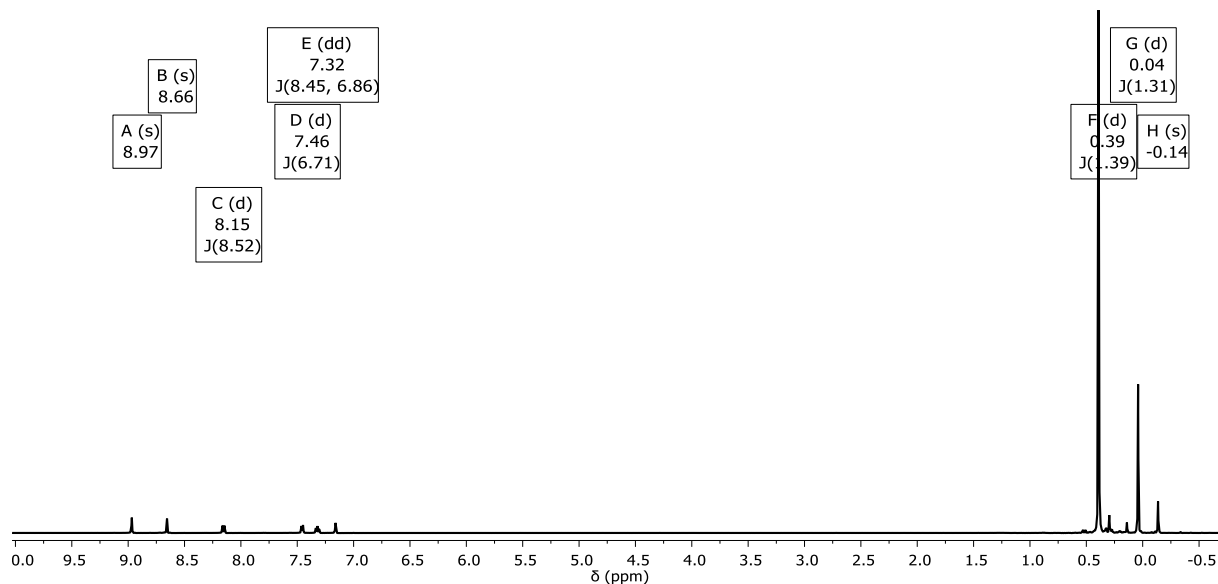


Figure S15: ^1H NMR spectrum of a solution of 1,5-Bis[2-bis(trimethylsilyl)methyl]aluminyl)-2-(trimethylsilyl)vinyl]-anthracene **7** in C_6D_6 (301 K, 500 MHz).

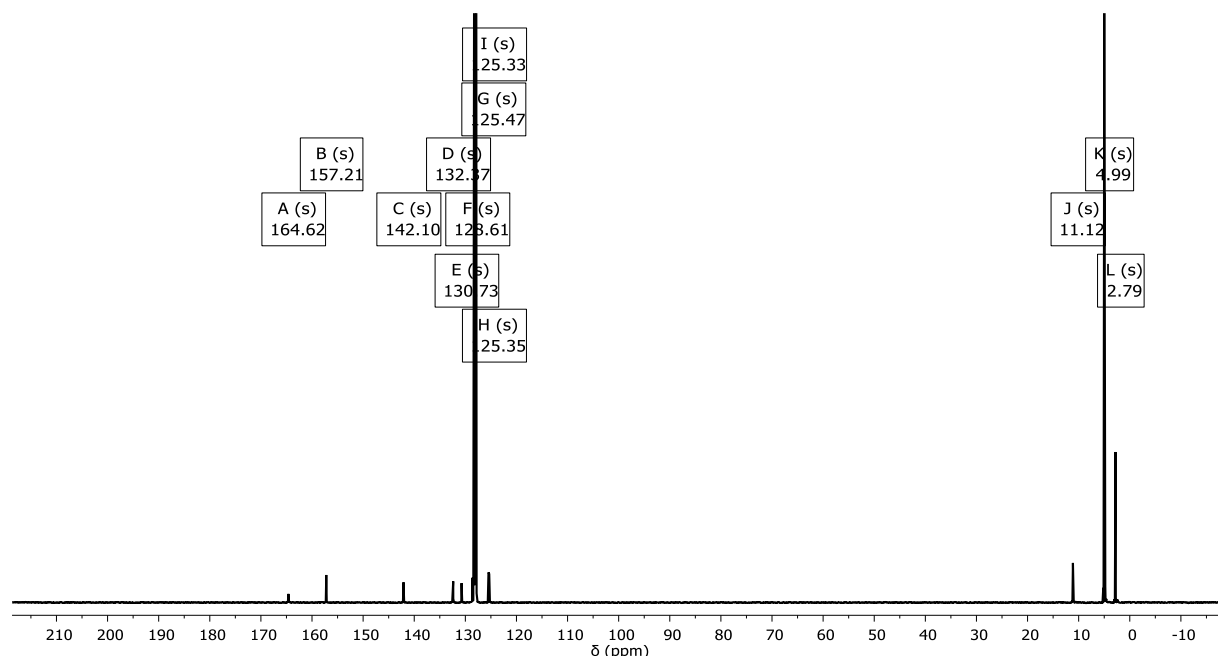


Figure S16: ^{13}C NMR spectrum of a solution of 1,5-Bis[2-bis(trimethylsilyl)methyl]aluminyl)-2-(trimethylsilyl)vinyl]-anthracene **7** in C_6D_6 (303 K, 126 MHz).

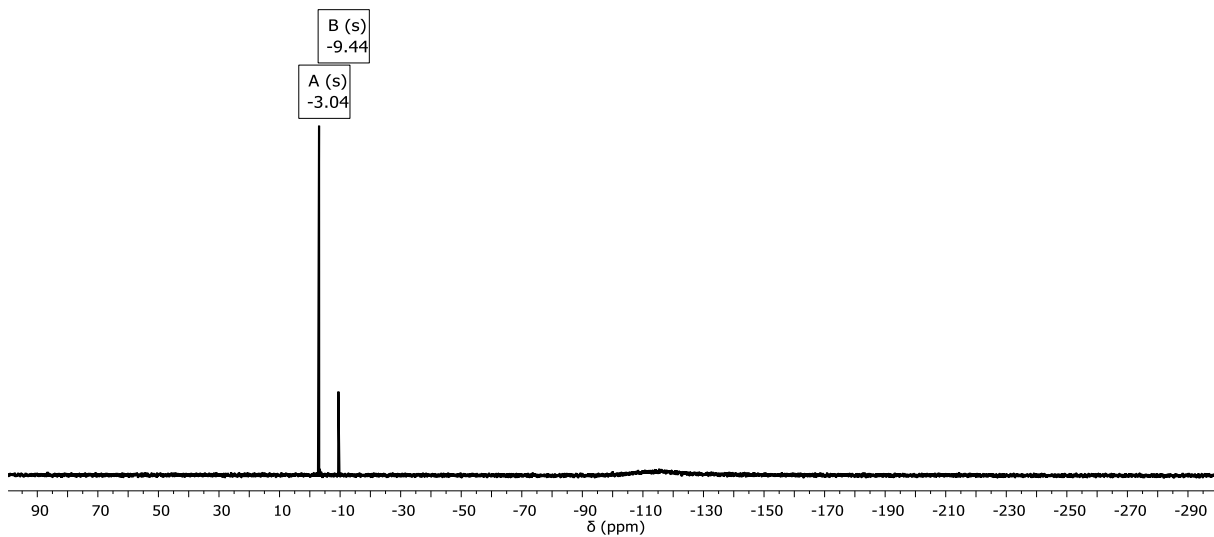


Figure S17: $^{29}\text{Si}\{\text{H}\}$ NMR spectrum of a solution of 1,5-Bis[2-bis(trimethylsilylmethyl)aluminyl]-2-(trimethylsilyl)vinyl]anthracene **7** in C_6D_6 (301 K, 500 MHz).

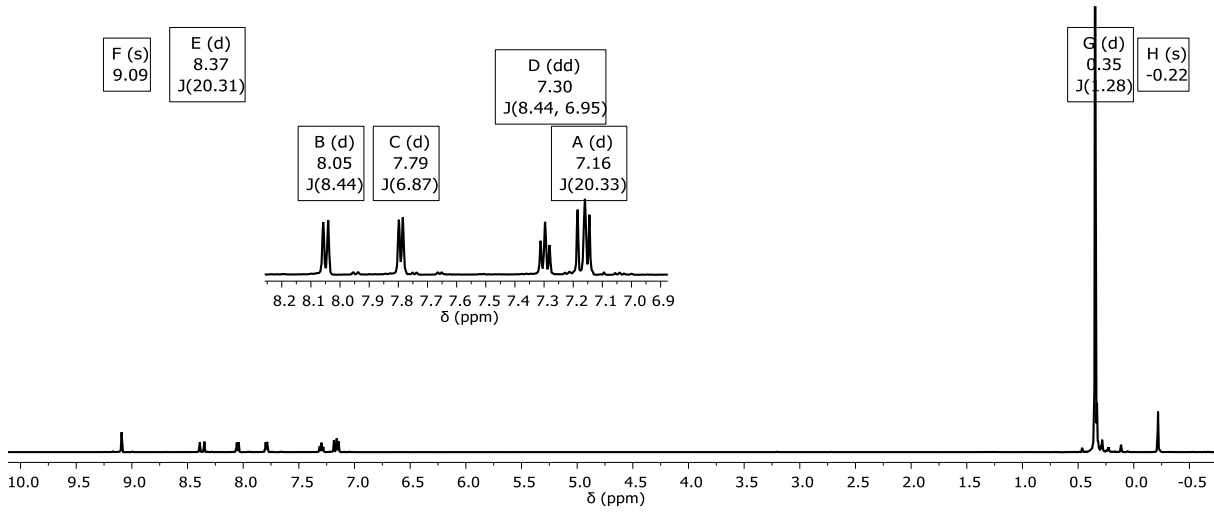


Figure S20: ^1H NMR spectrum of a solution of 1,5-Bis[2-bis(trimethylsilylmethyl)aluminyl]vinyl]anthracene **8** in C_6D_6 (301 K, 500 MHz).

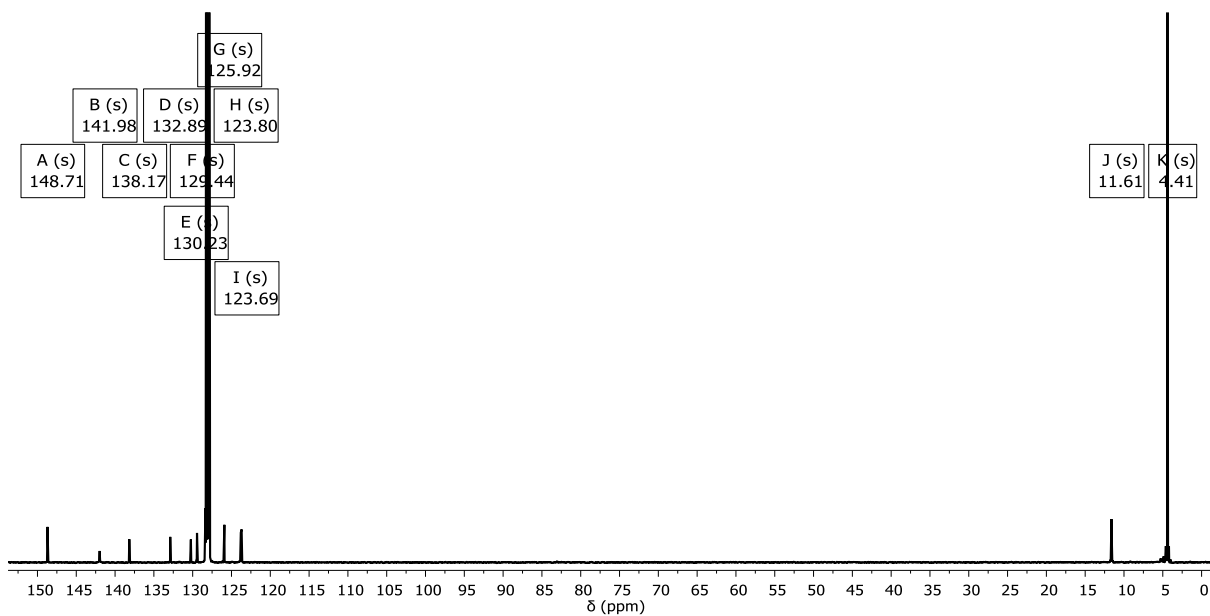


Figure S21: $^{13}\text{C}\{^1\text{H}\}$ NMR spectrum of a solution of 1,5-Bis[2-bis(trimethylsilylmethyl)aluminyl]vinyl]anthracene **8** in C_6D_6 (303 K, 126 MHz).

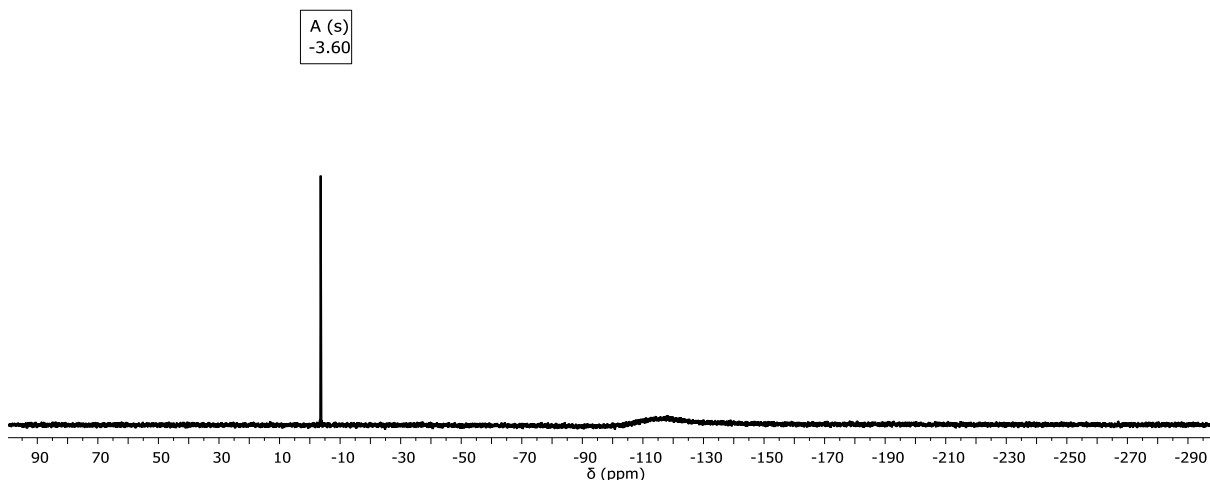


Figure S22: $^{29}\text{Si}\{^1\text{H}\}$ NMR spectrum of a solution of 1,5-Bis[2-bis(trimethylsilylmethyl)aluminyl]vinyl]anthracene **8** in C_6D_6 (301 K, 99 MHz).

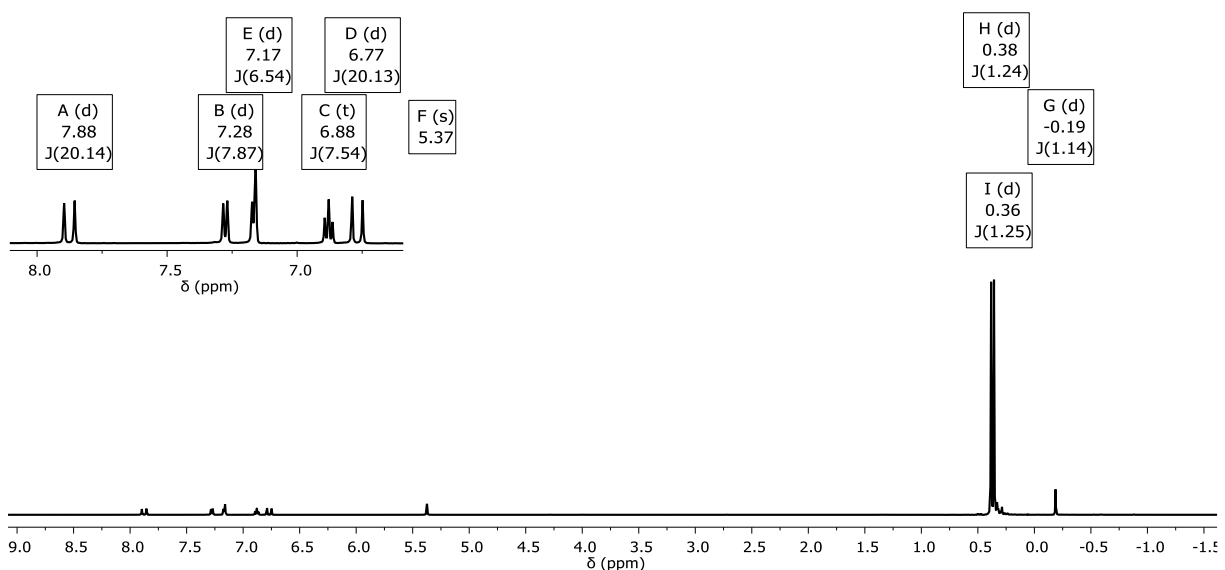


Figure S23: ^1H NMR spectrum of a solution of the *anti*-photo-dimer of **8** (*anti*-**9**) in C_6D_6 (302 K, 500 MHz).

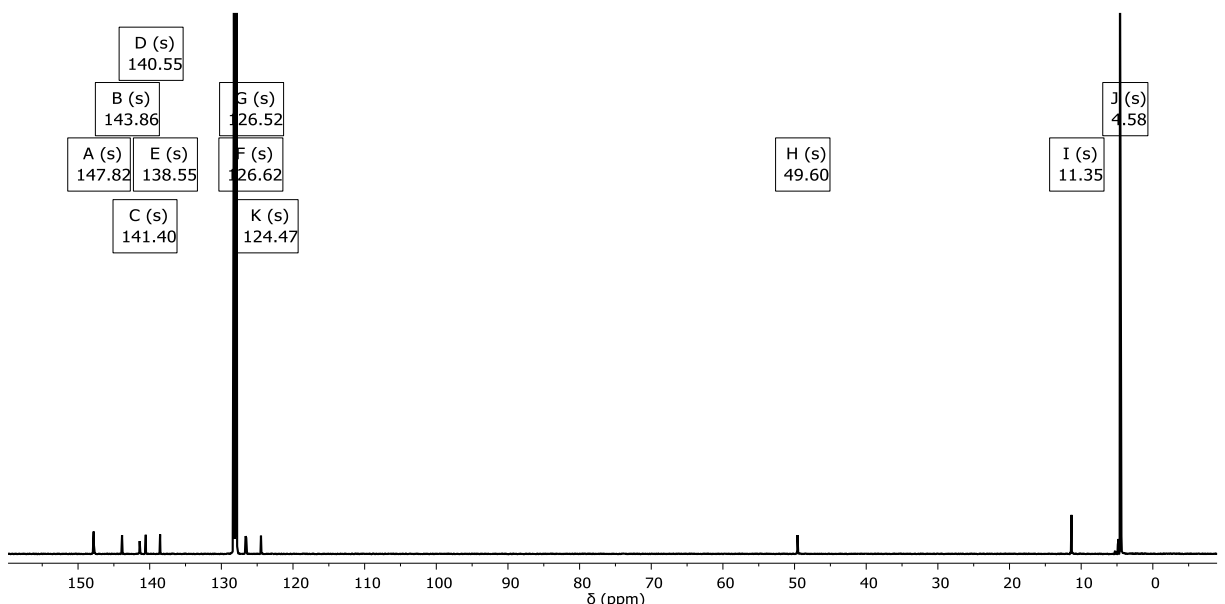


Figure S18: $^{13}\text{C}\{^1\text{H}\}$ NMR spectrum of a solution of the *anti*-photo-dimer of **8** (*anti*-**9**) in C_6D_6 (303 K, 126 MHz).

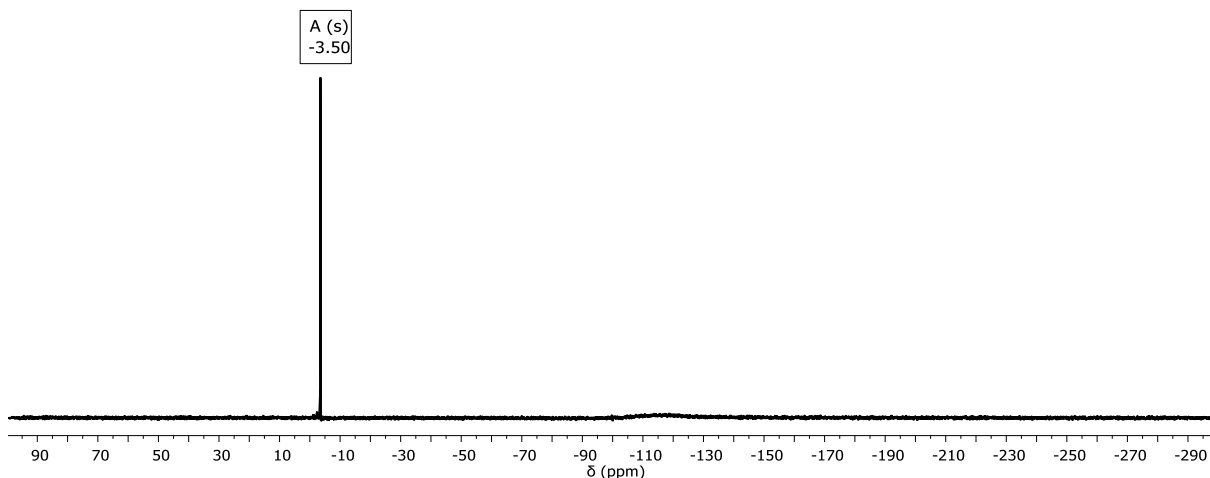


Figure S19: $^{29}\text{Si}\{\text{H}\}$ NMR spectrum of a solution of the *anti*-photo-dimer of **8** (*anti*-**9**) in C_6D_6 (301 K, 99 MHz).

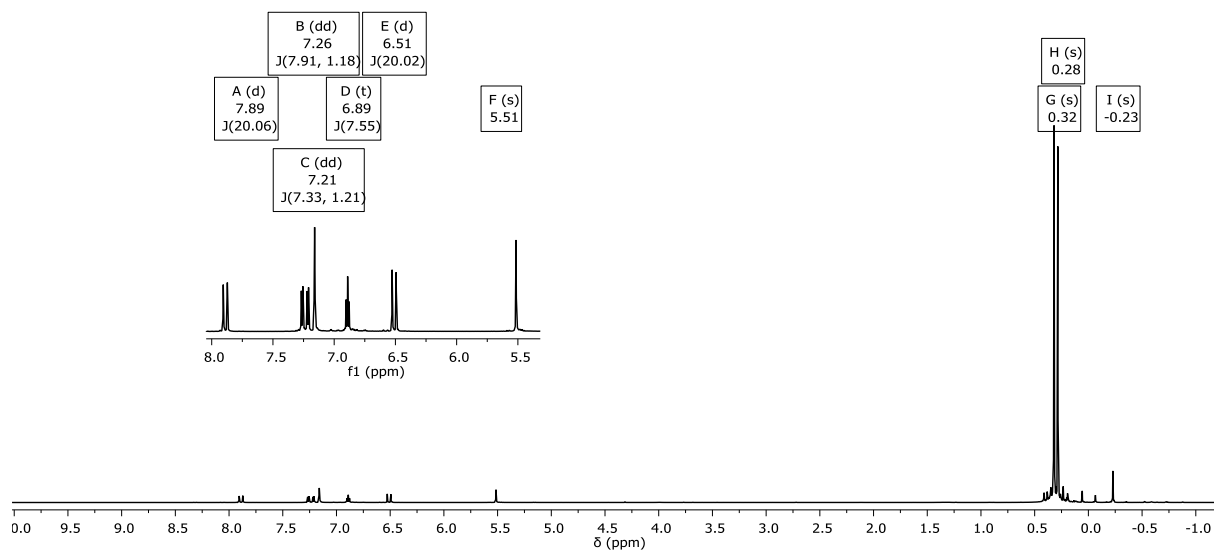


Figure S26: ^1H NMR spectrum of a solution of the *syn*-photo-dimer of **8** (*syn*-**9**) in C_6D_6 (313 K, 600 MHz).

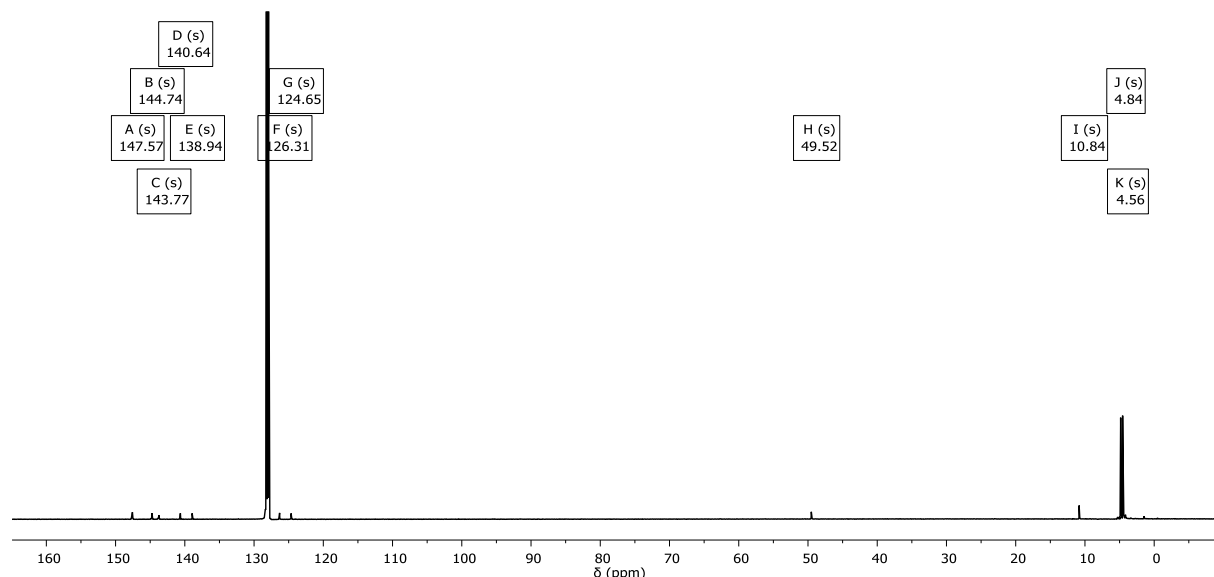


Figure S27: $^{13}\text{C}\{\text{H}\}$ NMR spectrum of a solution of the *syn*-photo-dimer of **8** (*syn*-**9**) in C_6D_6 (313 K, 126 MHz).

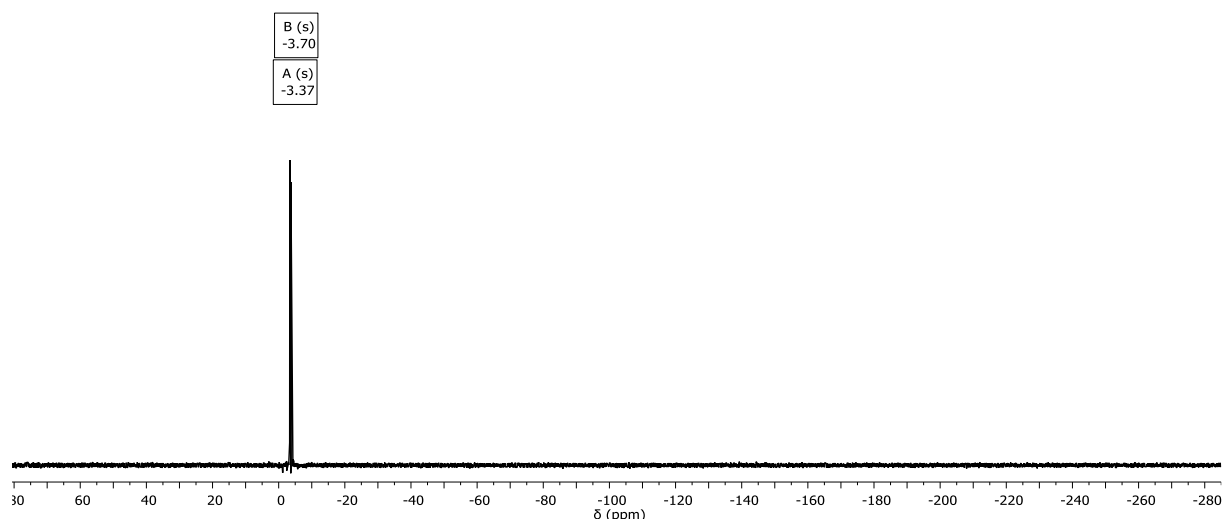


Figure S28: $^{29}\text{Si}\{\text{H}\}$ NMR spectrum of a solution of the *syn*-photo-dimer of **8** (*syn*-**9**) in C_6D_6 (313 K, 99 MHz).

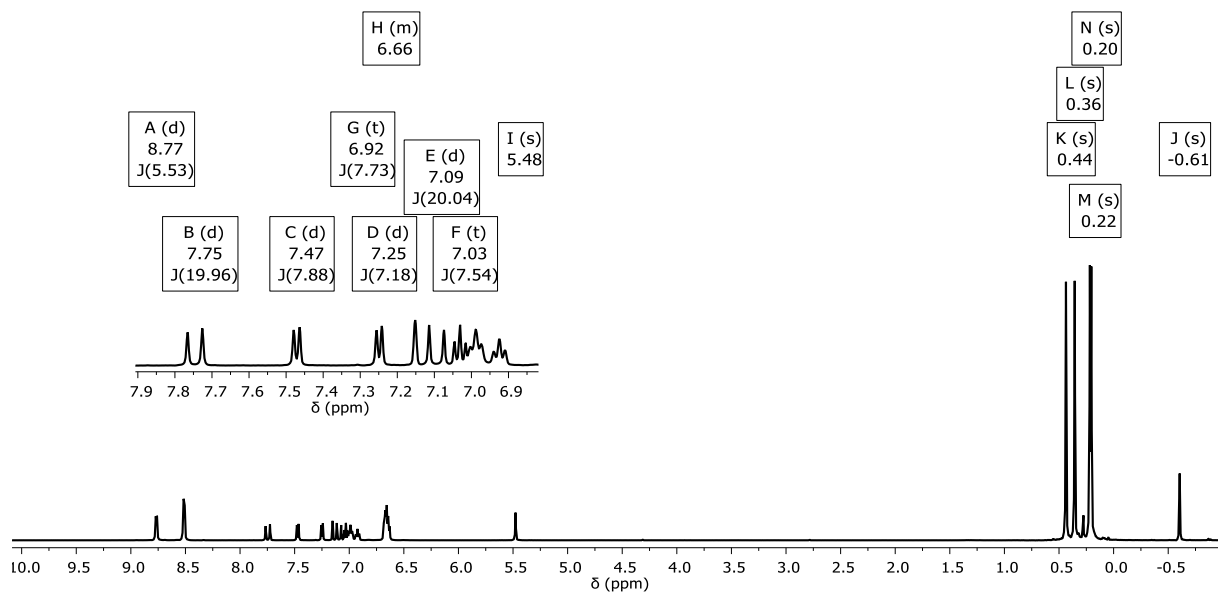


Figure S29: ^1H NMR spectrum of a solution of the fourfold pyridine adduct of *anti*-**9** (*anti*-**9**-Py₄) in C_6D_6 (302 K, 500 MHz).

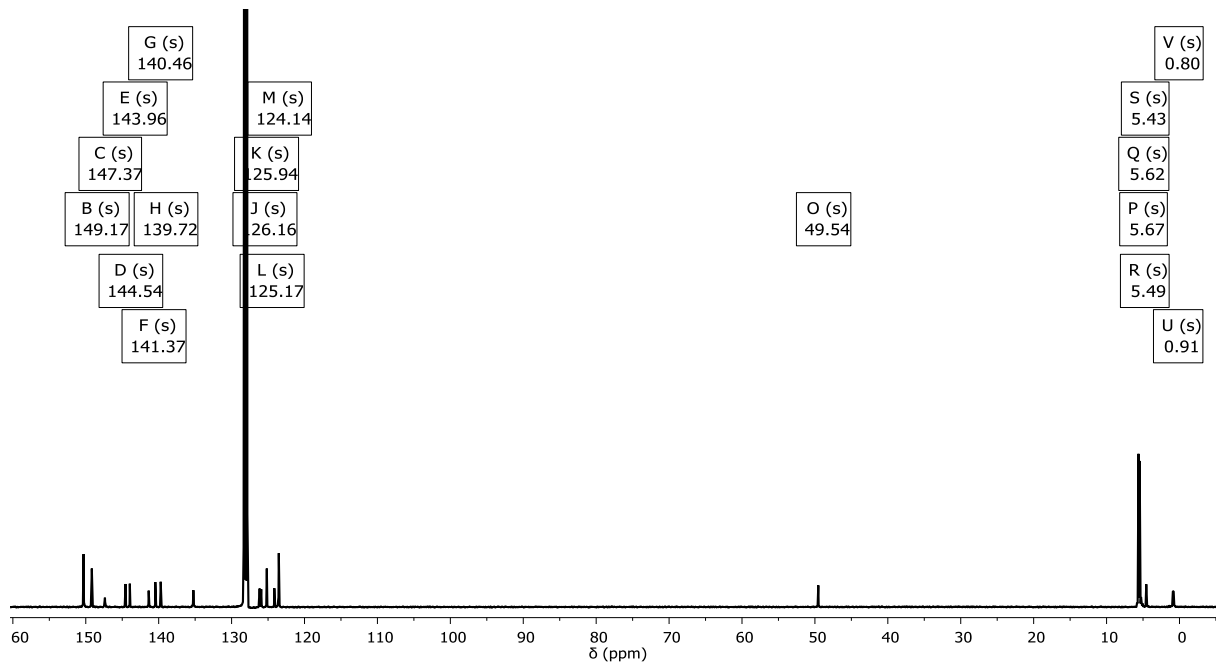


Figure S21: $^{13}\text{C}\{\text{H}\}$ NMR spectrum of a solution of the fourfold pyridine adduct of *anti*-9 (*anti*-9-Py₄) in C₆D₆ (303 K, 126 MHz).

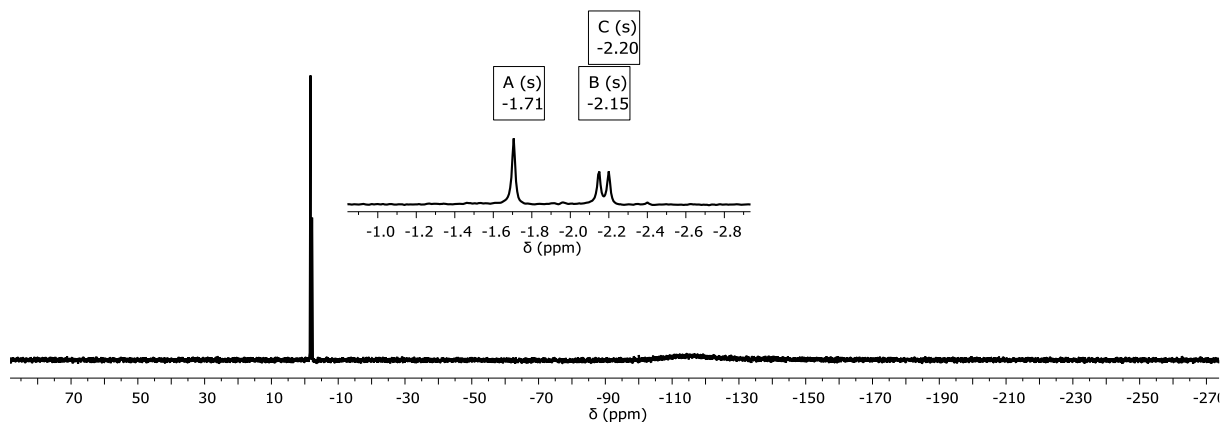


Figure S31: $^{29}\text{Si}\{\text{H}\}$ NMR spectrum of a solution of the fourfold pyridine adduct of *anti*-9 (*anti*-9-Py₄) in C₆D₆ (302 K, 99 MHz).

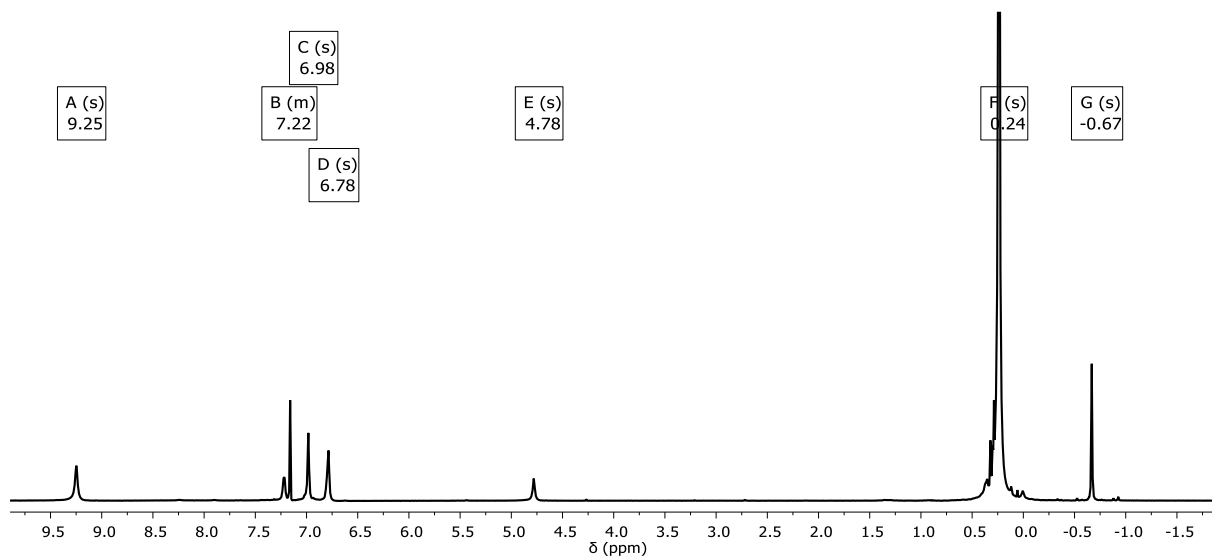


Figure S32: ^1H NMR spectrum of a solution of the twofold pyrazine adduct of anti-9 (anti-9-Pyz₂) in C₆D₆ (298 K, 500 MHz).

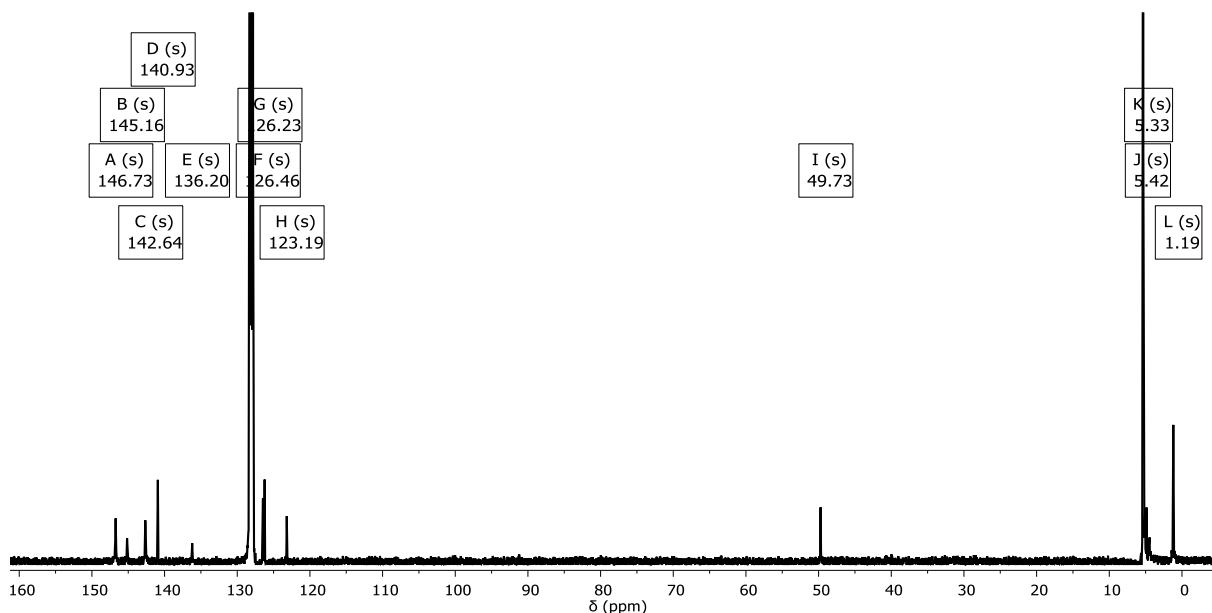


Figure S33: $^{13}\text{C}\{^1\text{H}\}$ NMR spectrum of a solution of the twofold pyrazine adduct of anti-9 (anti-9-Pyz₂) in C₆D₆ (298 K, 126 MHz).

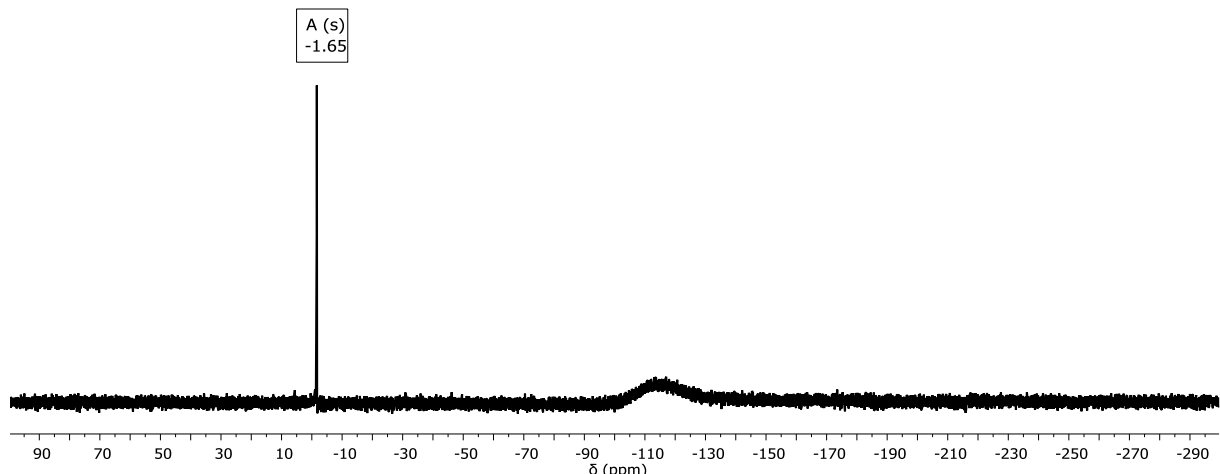


Figure S34: $^{29}\text{Si}\{\text{H}\}$ NMR spectrum of a solution of the twofold pyrazine adduct of anti-9 (anti-9-Pyz₂) in C₆D₆ (298 K, 99 MHz).

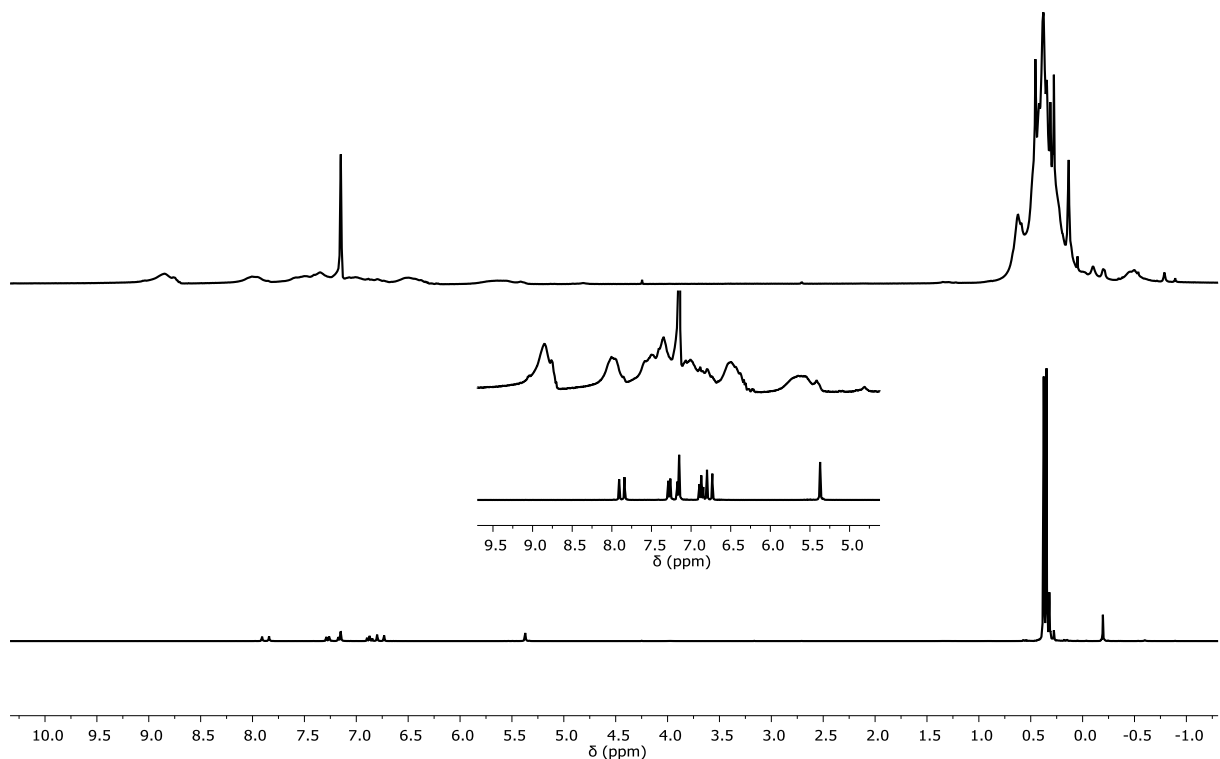


Figure S35: ^1H NMR spectrum of a solution of *anti*-9 with 2 equivalents of 4,4-bipyridine in C₆D₆ (298 K, 300 MHz).

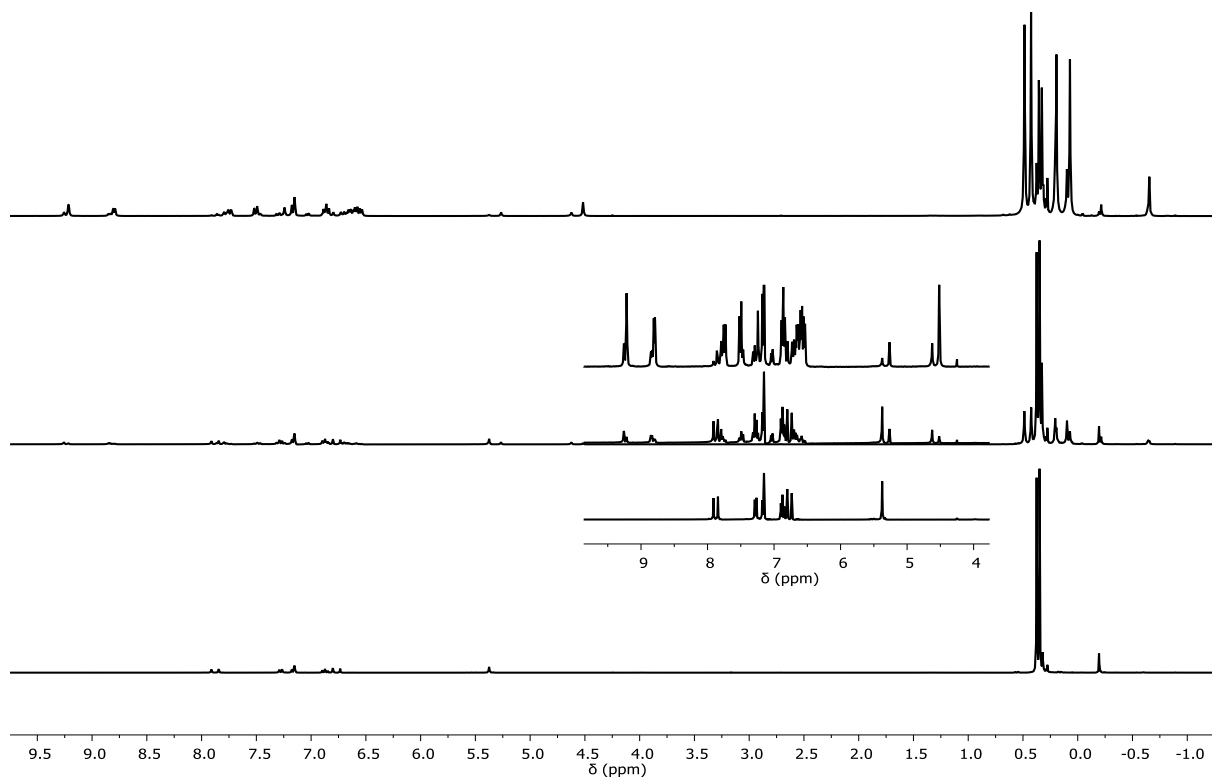


Figure S36: ^1H NMR spectra of a solution of *anti*-9 (bottom) with 1 equivalent (middle) and 2 equivalents (top) of 3,3'-bipyridine in C_6D_6 (298 K, 300 MHz).

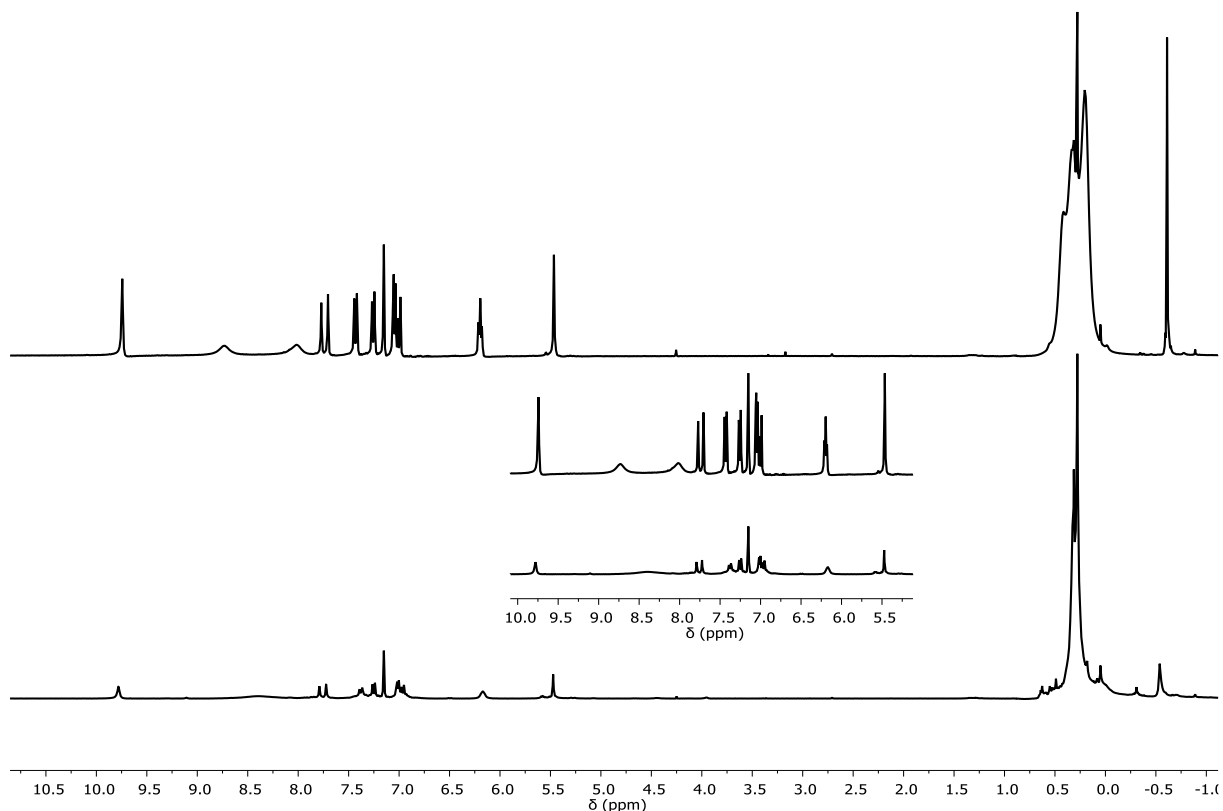


Figure S37: ^1H NMR spectra of a solution of *anti*-9 with 2 equivalents (bottom) and 4 equivalents (top) of pyrimidine in C_6D_6 (298 K, 300 MHz).

Crystallographic Data

Crystal Structure determination: Suitable crystals were obtained by slow evaporation of saturated solutions from ethyl acetate (anthracene-1,5-diyl bis(trifluoromethanesulfonate) not described in the article and herein referred to as **A**,³, *n*-pentane (*anti*-**4**; not discussed in detail in the article), dichloromethane (*anti*-**5**, *syn*-**5**), *N,N*-dimethylformamide (*syn*-**6**), toluene (**7**), *n*-hexane (**8**) benzene (*syn*-**9**, *anti*-**9**), or slowly grown from benzene (*anti*-**9**-Py₄, *anti*-**9**-Pyz₂) after adding the corresponding base to the solution of the tetraalane in benzene. The crystals were selected, coated with PARATONE-N oil, mounted on a glass fibre and transferred onto the goniometer of the diffractometer into a nitrogen gas cold stream, which immediately solidifies the oil. Data collection was performed on a Rigaku SuperNova diffractometer. Using Olex2,^[1] the structures were solved with the SHELXT^[2]structure solution program and except **A** refined with the SHELXL^[3] refinement package. **A** was refined with the olex2.refine [3] refinement package using Gauss-Newton minimization and NoSpherA2,^[4] an implementation of NOn-SPHERical Atom-form-factors in Olex2. NoSpherA2 implementation of HAR makes use of tailor-made aspherical atomic form factors calculated on-the-fly from a Hirshfeld-partitioned electron density (ED) – not from spherical-atom form factors. The ED is calculated from a Gaussian basis set single determinant SCF wave function – either Hartree-Fock or DFT using selected functionals - for a fragment of the crystal. This fragment can be embedded into an electrostatic crystal field by employing cluster charges or modelled using implicit solvation models, depending on the software used. The following options were used: SOFTWARE: ORCA PARTITIONING: NoSpherA2 INT ACCURACY: Normal METHOD: M062X BASIS SET: def2-TZVPP CHARGE: 0 MULTIPLICITY: 1

Crystal and refinement details, as well as CCDC numbers are provided in Tables S1 and S2. CCDC 2163879-2163889, and 2180919 contain the supplementary crystallographic data for this paper. These data can be obtained free of charge from The Cambridge Crystallographic Data Centre via <http://www.ccdc.cam.ac.uk/conts/retrieving.html>

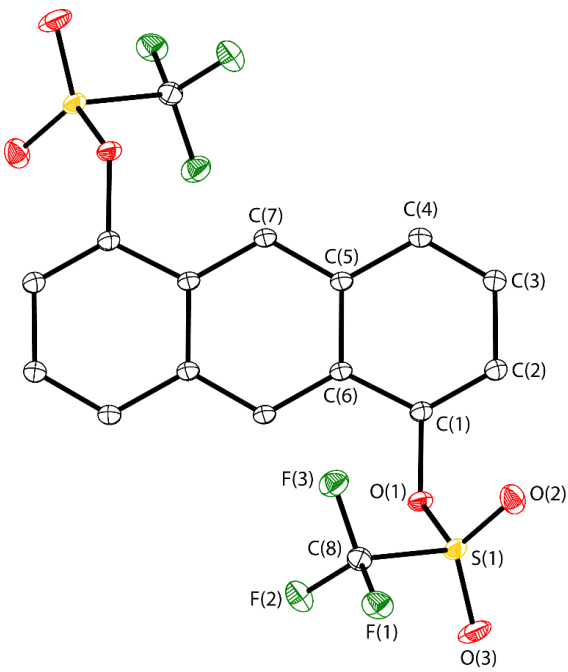


Figure S38: Molecular structure of **A** in the solid state. Displacement ellipsoids are drawn at the 50% probability level. Hydrogen atoms are omitted for clarity. Symmetry code $1-x$, $1-y$, $1-z$ for E' . Selected bond lengths [\AA] and angles [$^\circ$]: C(1)–O(1) 1.4232(5), O(1)–S(1) 1.5691(4), S(1)–O(2) 1.4158(4), S(1)–O(3) 1.4162(4), S(1)–C(8) 1.8367(5), C(8)–F(3) 1.3220(6); C(6)–C(1)–C(2) 123.71(4), C(6)–C(1)–O(1) 116.30(4), C(2)–C(1)–O(1) 119.83(4), O(1)–S(1)–O(2) 112.08(2), O(2)–S(1)–O(3) 122.63(3), O(1)–S(1)–C(8) 101.33(2), F(1)–C(8)–F(2) 109.28(4), F(1)–C(8)–F(3) 109.63(4), F(2)–C(8)–F(3) 109.60(4).

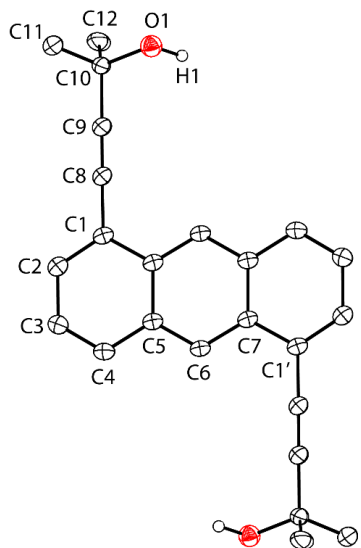


Figure S39a: Molecular structure of **3** (one molecule of the asymmetric unit for simpler representation of bond lengths and angles. For further molecules see Figure 33b) in the solid state. Displacement ellipsoids are drawn at the 40% probability level. Hydrogen atoms (except OH groups) are omitted for clarity. Symmetry code $2-x$, $2-y$, $1-z$ for E' . Selected bond lengths [\AA] and angles [$^\circ$]: O(1)–C(10) 1.442(1), C(1)–C(2) 1.369(2), C(1)–C(8) 1.439(1), C(8)–C(9) 1.193(2), C(9)–C(10) 1.483(1); C2–C1–C7' 120.0(1), C2–C1–C8 121.1(1), C(8)–C(1)–C(7') 118.9(1), C(1)–C(8)–C(9) 177.3(1), C(8)–C(9)–C(10) 178.4(2).

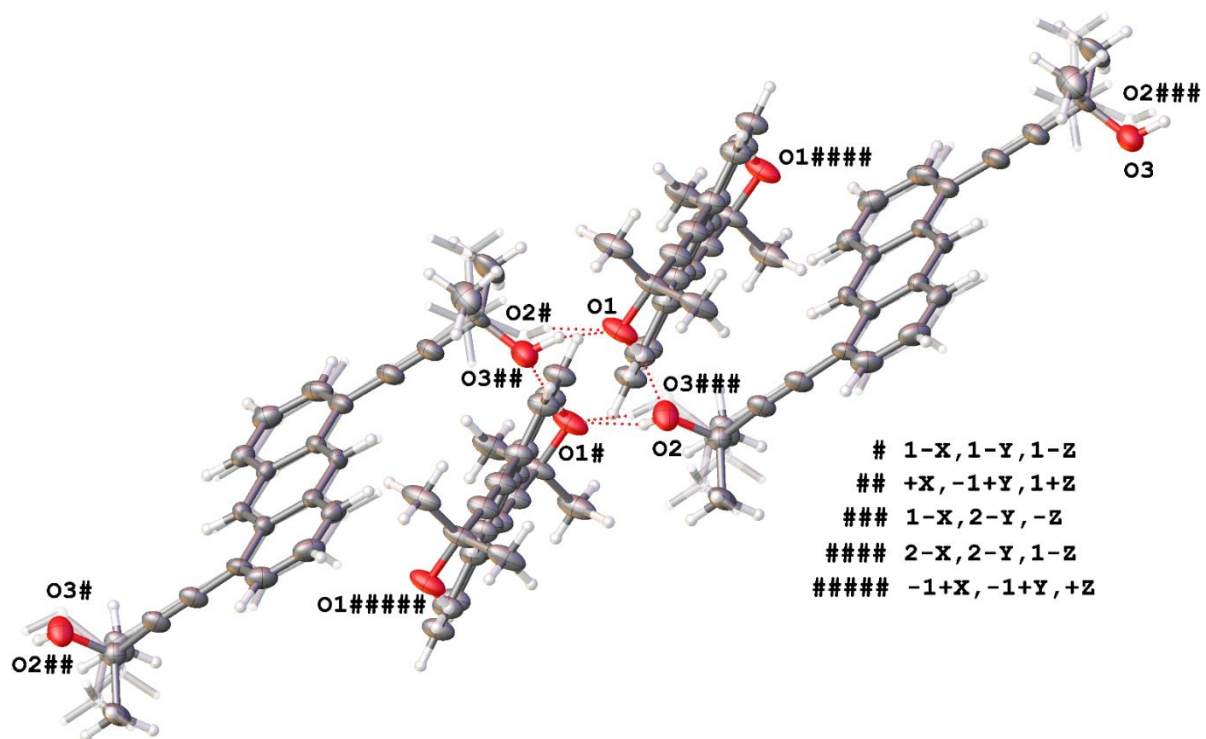


Figure S39b: Molecular structure of 3 showing the arrangement of the non-disordered molecule containing O1 and the 1:1 disordered molecule containing O2 and O3. Both molecules are arranged at a centre of inversion, the first one obeys this symmetry, the second one does not. One part of the disordered molecule is shown in translucent grey.

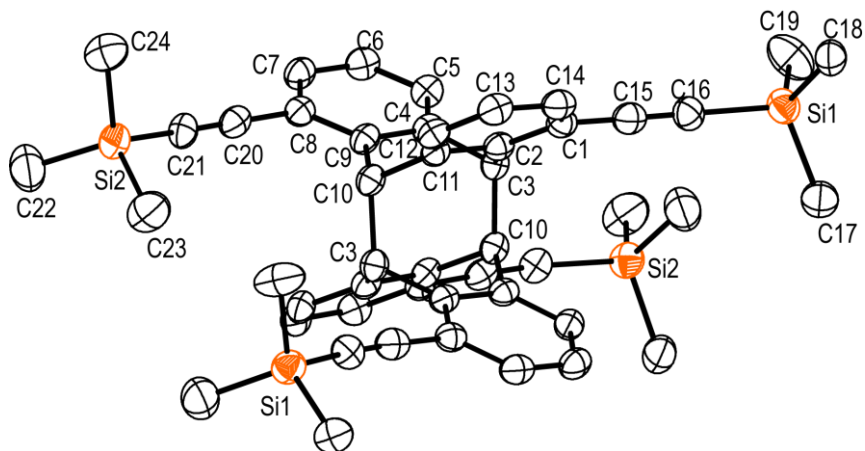


Figure S40: Molecular structure of the all-S isomer of *anti*-4 in the crystalline state. Displacement ellipsoids are drawn at the 40% probability level. H atoms are omitted for clarity. Symmetry code 3/2-x, 1/2-y, +z for E'. Selected bond lengths [Å] and angles [°]: C(7)-C(8) 1.403(4), C(8)-C(20) 1.437(4), C(9)-C(10) 1.517(4), C(10)-C(3') 1.603(4), C(20)-C(21) 1.201(5), Si(2)-C(21) 1.846(3), Si(2)-C(22) 1.841(4); C(7)-C(8)-C(9) 119.4(3), C(7)-C(8)-C(20) 121.3(3), C(8)-C(9)-C(10) 123.3(3), C(8)-C(20)-C(21) 176.3(3), C(9)-C(10)-C(3') 113.2(2), C(9)-C(10)-C(11) 107.6(2), C(20)-C(21)-Si(2) 169.6(3), C(21)-Si(2)-C(22) 111.1(2).

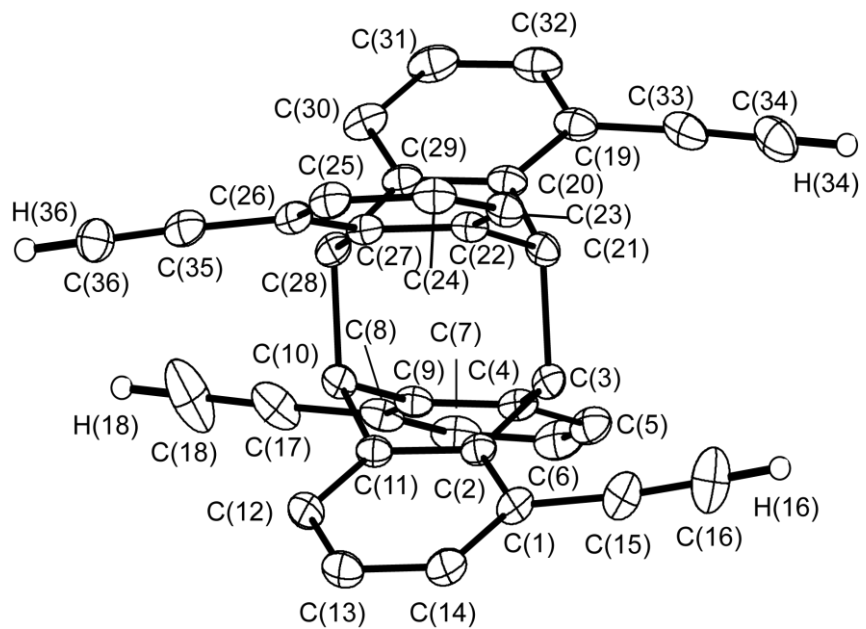


Figure S41: Molecular structure of the all-*R* isomer of *anti*-5 in the crystalline state. Displacement ellipsoids are drawn at the 40% probability level. H atoms (except H(16), H(18), H(34) and H(36)) are omitted for clarity. Selected bond lengths [\AA] and angles [$^\circ$]: C(1)–C(14) 1.401(3), C(1)–C(2) 1.400(2), C(1)–C(15) 1.438(3), C(15)–C(16) 1.190(3), C(17)–C(18) 1.181(3), C(33)–C(34) 1.193(3), C(35)–C(36) 1.188(3), C(2)–C(1)–C(14) 119.48(17), C(2)–C(1)–C(15) 119.29(17), C(1)–C(15)–C(16) 175.5(2), C(8)–C(17)–C(18) 176.6(2).

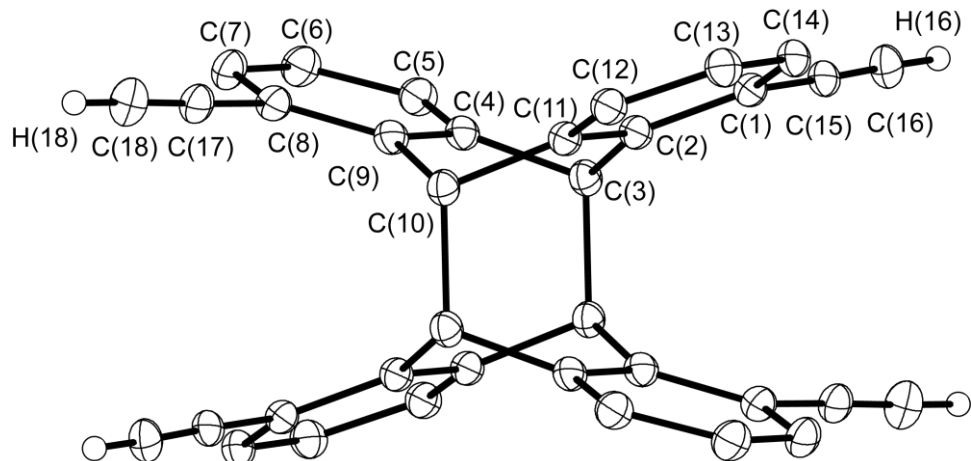


Figure S42: Molecular structure of *syn*-5 in the crystalline state. Displacement ellipsoids are drawn at the 40% probability level. H atoms (except H(16), H(18), H(16') and H(18')) are omitted for clarity. 1– x , 1– y , 1– z . Selected bond lengths [\AA] and angles [$^\circ$]: C(1)–C(2) 1.405(2), C(1)–C(14) 1.403(2), C(1)–C(15) 1.439(2), C(15)–C(16) 1.196(2), C(8)–C(7) 1.404(2), C(8)–C(9) 1.406(2), C(8)–C(17) 1.436(2), C(17)–C(18) 1.192(2); C(2)–C(1)–C(14) 119.5(1), C(14)–C(1)–C(15) 119.5(1), C(2)–C(1)–C(15) 121.0(1), C(1)–C(15)–C(16) 178.2(1), C(7)–C(8)–C(9) 119.4(1), C(7)–C(8)–C(17) 118.9(1), C(9)–C(8)–C(17) 121.7(1), C(8)–C(17)–C(18) 176.8(1).

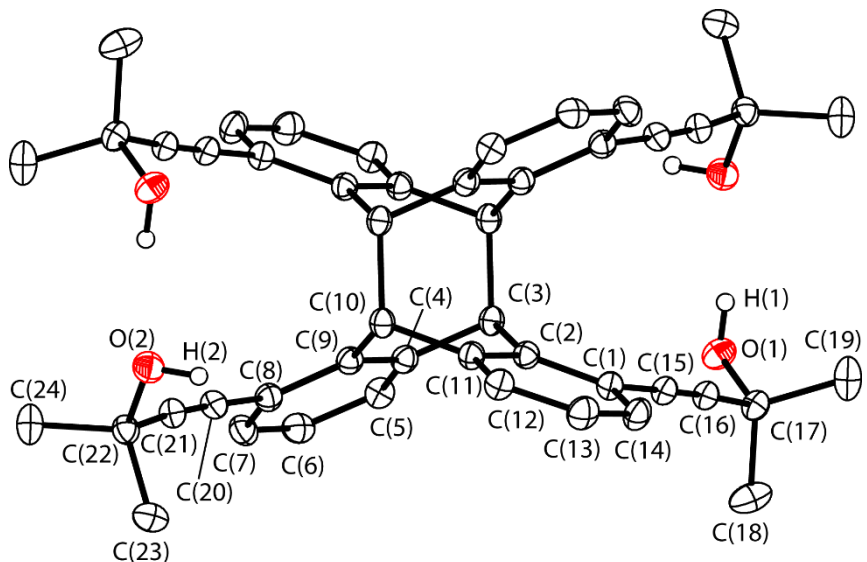


Figure S43: Molecular structure of *syn*-6 in the crystalline state. Displacement ellipsoids are drawn at the 50% probability level. H atoms (except H(1), H(2), H(1') and H(2')) are omitted for clarity. Symmetry code: 1-x, -y, 1-z for E'. Selected bond lengths [Å] and angles [°]: O(1)-C(17) 1.444(2), O(2)-C(22) 1.438(2), C(1)-C(2) 1.407(2), C(1)-C(15) 1.435(2), C(15)-C(16) 1.202(3), C(16)-C(17) 1.475(3), C(8)-C(20) 1.433(2), C(20)-C(21) 1.202(3), C(21)-C(22) 1.478(2); C(2)-C(1)-C(15) 119.6(2), C(14)-C(1)-C(2) 119.2(2), C(14)-C(1)-C(15) 121.3(2), C(1)-C(15)-C(16) 176.3(2), C(15)-C(16)-C(17) 177.4(2), C(7)-C(8)-C(9) 119.4(2), C(7)-C(8)-C(20) 120.7(2), C(9)-C(8)-C(20) 119.8(2), C(8)-C(20)-C(21) 175.9(2), C(20)-C(21)-C(22) 175.3(2).

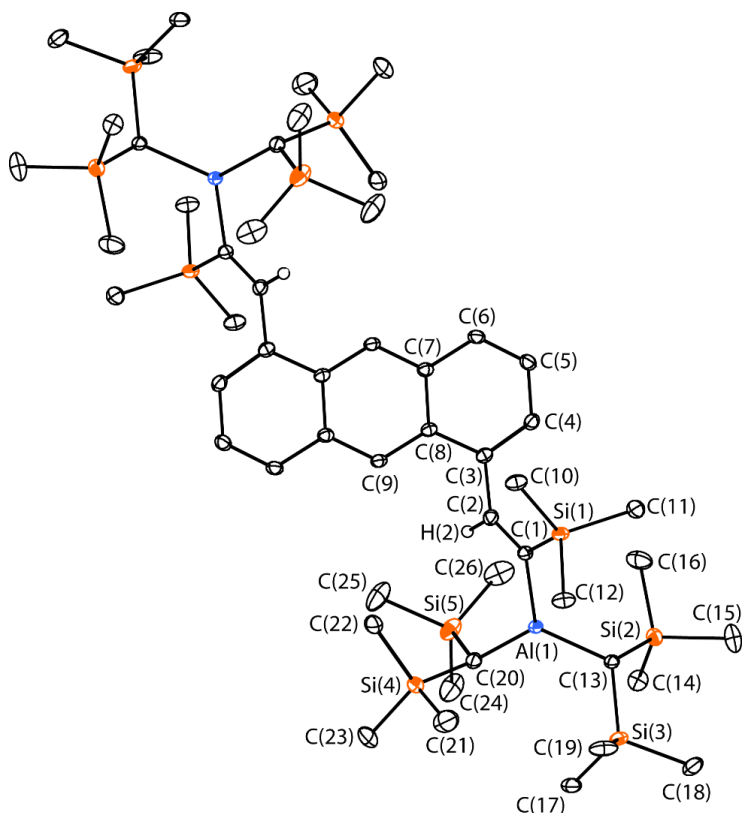


Figure S44: Molecular structure of 7 in the crystalline state. Displacement ellipsoids are drawn at the 40% probability level. H atoms (except H(2) and H(2')) are omitted for clarity. Symmetry code: 1-x, 1-y, 1-z for E'. Selected bond lengths [Å] and angles [°]: C(1)-C(2) 1.349(2), C(2)-C(3) 1.485(2), C(1)-Al(1) 1.965(1), Al(1)-C(13) 1.969(1), Al(1)-C(20) 1.957(1), C(1)-Si(1) 1.880(1), C(13)-Si(2) 1.875(1), C(20)-Si(4) 1.879(2); C(3)-C(2)-C(1) 127.2(1), C(2)-C(1)-Al(1) 113.6(1), C(2)-C(1)-Si(1) 123.5(1), Si(1)-C(1)-Al(1) 122.9(1), C(20)-Al(1)-C(13) 122.1(1), C(1)-Al(1)-C(13) 117.5(1), C(1)-Al(1)-C(20) 120.3(6).

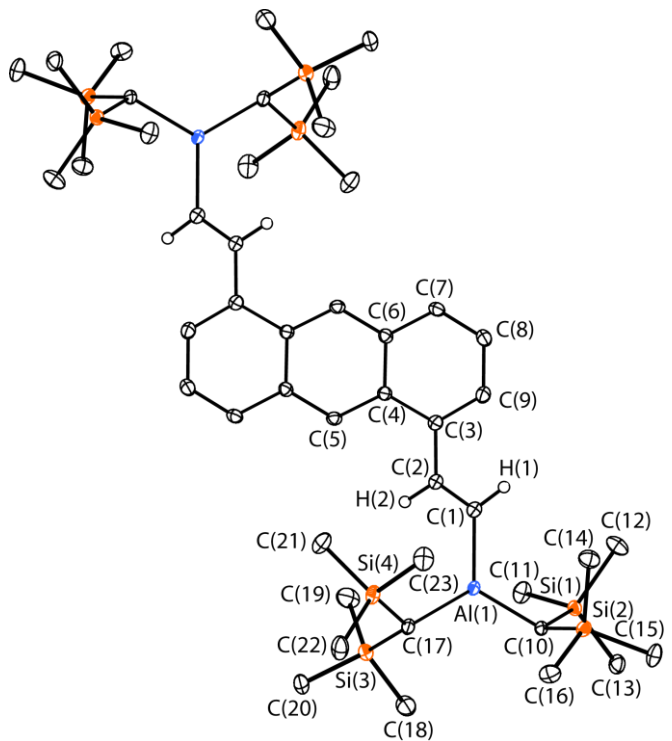


Figure S45: Molecular structure of **8** in the crystalline state. Displacement ellipsoids are drawn at the 40% probability level. H atoms (except H(1), H(2), H(1'), H(2')) are omitted for clarity. Symmetry code: $1-x, 1-y, 1-z$ for E' . Selected bond lengths [\AA] and angles [$^\circ$]: C(1)–C(2) 1.339(2), C(1)–Al(1) 1.954(2), C(2)–C(3) 1.479(2), Al(1)–C(10) 1.950(1), Al(1)–C(17) 1.950(2); C(3)–C(2)–C(1) 126.22(14), C(2)–C(1)–Al(1) 124.52(12), C(1)–Al(1)–C(10) 118.66(6) C(10)–Al(1)–C(17) 119.73(6), C(1)–Al(1)–C(17) 121.60(6).

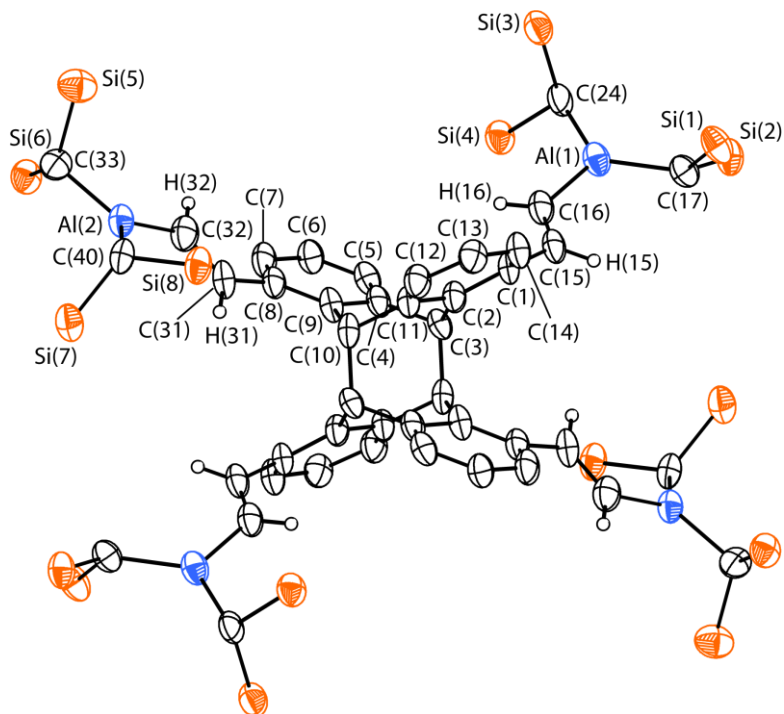


Figure S46: Molecular structure of *syn*-**9** in the crystalline state. Displacement ellipsoids are drawn at the 40% probability level. H atoms (except vinylic H atoms) are omitted for clarity. Symmetry code: $1-x, -y, 1-z$ for E' . Selected bond lengths [\AA] and angles [$^\circ$]: C(1)–C(15) 1.499(9), C(15)–C(16) 1.341(10), Al(1)–C(16) 1.940(8), Al(1)–C(17) 1.960(7), Al(1)–C(24) 1.950(7), C(8)–C(31) 1.486(9), C(31)–C(32) 1.338(10), Al(2)–C(32) 1.938(8), Al(2)–C(33) 1.957(7), Al(2)–C(40) 1.950(7); C(1)–C(15)–C(16) 124.2(6), C(15)–C(16)–Al(1) 128.6(5), C(16)–Al(1)–C(24) 116.6(3), C(16)–Al(1)–C(17) 119.9(3), C(17)–Al(1)–C(24) 123.5(3), C(8)–C(31)–C(32) 125.0(7), C(31)–C(32)–Al(2) 129.3(6), C(32)–Al(2)–C(33) 117.1(3), C(32)–Al(2)–C(40) 123.7(3), C(33)–Al(2)–C(40) 119.1(3).

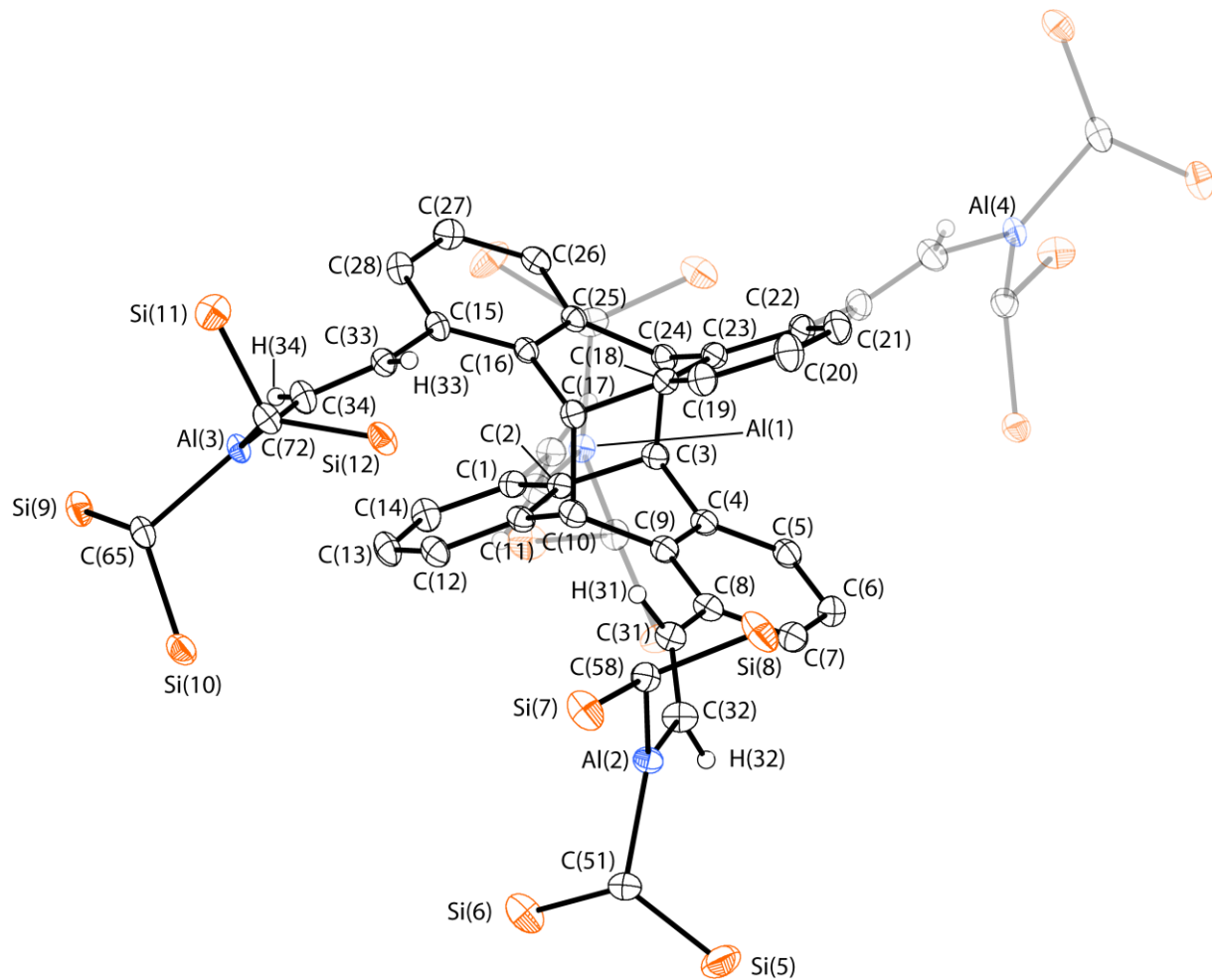


Figure S47: Molecular structure of *anti*-9 in the crystalline state. Displacement ellipsoids are drawn at the 40% probability level. H atoms (except vinylic H atoms) are omitted for clarity. Selected bond lengths [Å] and angles [°]: C(8)–C(31) 1.488(3), C(31)–C(32) 1.331(3), C(32)–Al(2) 1.951(3), C(15)–C(33) 1.479(3), C(33)–C(34) 1.340(3), C(34)–Al(3) 1.950(2); C(8)–C(31)–C(32) 125.0(2), C(31)–C(32)–Al(2) 129.6(2), C(32)–Al(2)–C(51) 116.8(1), C(32)–Al(2)–C(58) 119.1(1), C(51)–Al(2)–C(58) 124.1(1), C(15)–C(33)–C(34) 125.8(2), C(33)–C(34)–Al(3) 123.4(2), C(34)–Al(3)–C(65) 120.5(1), C(34)–Al(3)–C(72) 121.4(1), C(65)–Al(3)–C(72) 118.1(1).

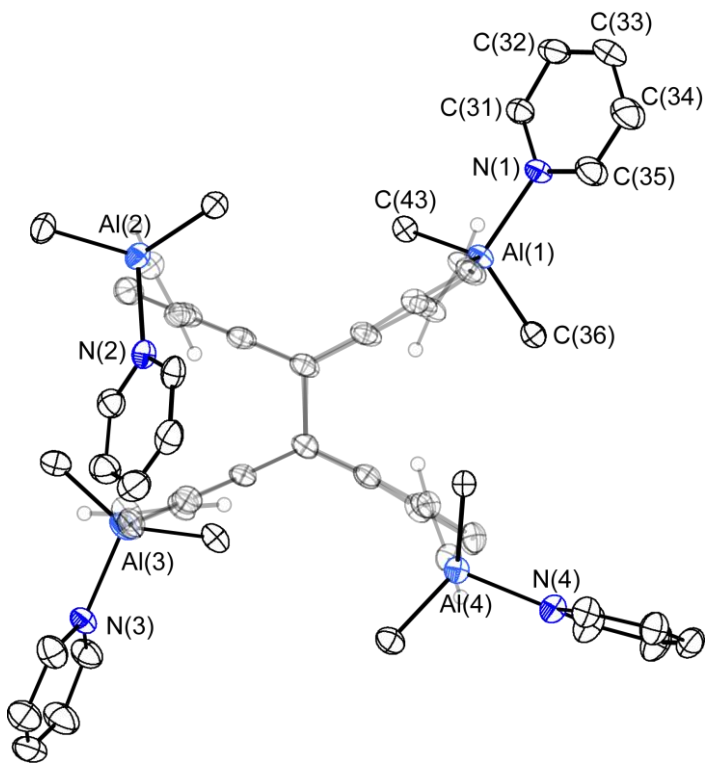
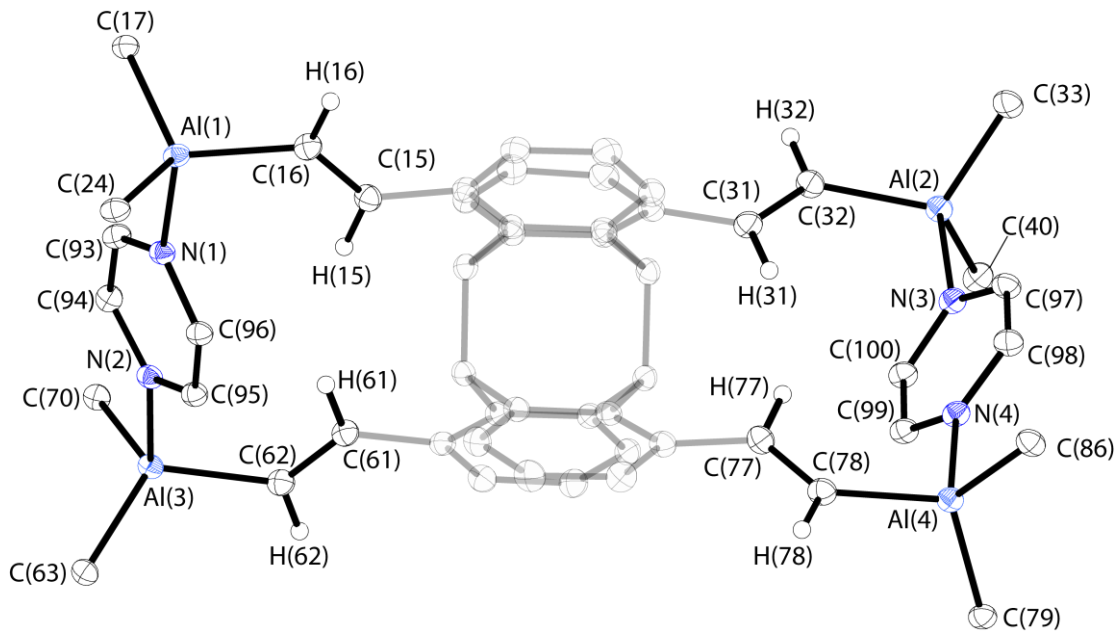


Figure S48: Molecular structure of *anti*-9•Py₄ in the crystalline state. Displacement ellipsoids are drawn at the 40% probability level. H atoms (except vinylic H atoms which are greyed out) and trimethylsilyl groups are omitted for clarity. Selected bond lengths [Å] and angles [°]: Al(1)–N(1) 2.030(2), Al(2)–N(2) 2.033(2), Al(3)–N(3) 2.019(2), Al(4)–N(4) 2.036(2); C(31)–N(1)–C(35) 117.1(2), C(31)–N(1)–Al(1) 122.2(2), C(35)–N(1)–Al(1) 120.0(2), C(30)–Al(1)–N(1) 93.15(10), C(30)–Al(1)–C(36) 115.6(1), C(30)–Al(1)–C(43) 118.7(1), C(36)–Al(1)–N(1) 112.7(1), C(43)–Al(1)–N(1) 105.1(1), C(43)–Al(1)–C(36) 109.9(1).



FigureS49: Molecular structure of *anti*-9-PyZ₂ in the crystalline state. Displacement ellipsoids are drawn at the 40% probability level. H atoms (except vinylic hydrogen atoms which are greyed out) and SiMe₃ groups are omitted for clarity. Selected bond lengths [Å] and angles [°]: C(15)–C(16) 1.338(3), C(31)–C(32) 1.335(3), C(61)–C(62) 1.342(3), C(77)–C(78) 1.335(3), Al(1)–N(1) 2.119(2), Al(2)–N(3) 2.116(2), Al(3)–N(2) 2.117(2), Al(4)–N(4) 2.108(2); C(16)–Al(1)–C(17) 110.9(1), C(16)–Al(1)–C(24) 115.9(1), C(16)–Al(1)–N(1) 101.2(1), C(17)–Al(1)–C(24) 120.1(1), C(17)–Al(1)–N(1) 102.1(1), C(24)–Al(1)–N(1) 103.3(1), Al(1)–N(1)–C(93) 121.7(1), Al(1)–N(1)–C(96) 122.0(1), C(93)–N(1)–C(96) 116.3(2), C(32)–Al(2)–C(33) 110.6(1), C(32)–Al(2)–C(40) 114.0(1), C(32)–Al(2)–N(3) 101.7(1), C(33)–Al(2)–C(40) 121.3(1), C(33)–Al(2)–N(3) 102.6(1), C(40)–Al(2)–N(3) 103.7(1), Al(2)–N(3)–C(97) 122.3(1), Al(2)–N(3)–C(100) 120.9(1), C(97)–N(3)–C(100) 116.7(2), C(62)–Al(3)–C(63) 115.1(1), C(62)–Al(3)–C(70) 113.3(1), C(62)–Al(3)–N(2) 98.9(1), C(63)–Al(3)–C(70) 118.3(1), C(63)–Al(3)–N(2) 103.8(1), C(70)–Al(3)–N(2) 104.1(1), Al(3)–N(2)–C(94) 122.1(1), Al(3)–N(2)–C(95) 121.4(1), C(94)–N(2)–C(95) 116.4(2), C(78)–Al(4)–C(79) 112.3(1), C(78)–Al(4)–C(86) 114.8(1), C(78)–Al(4)–N(4) 100.1(1), C(79)–Al(4)–C(86) 119.8(1), C(79)–Al(4)–N(4) 102.5(1), C(86)–Al(4)–N(4) 103.9(1), Al(4)–N(4)–C(98) 124.0(1), Al(4)–N(4)–C(99) 118.9(1), C(98)–N(4)–C(99) 117.1(2).

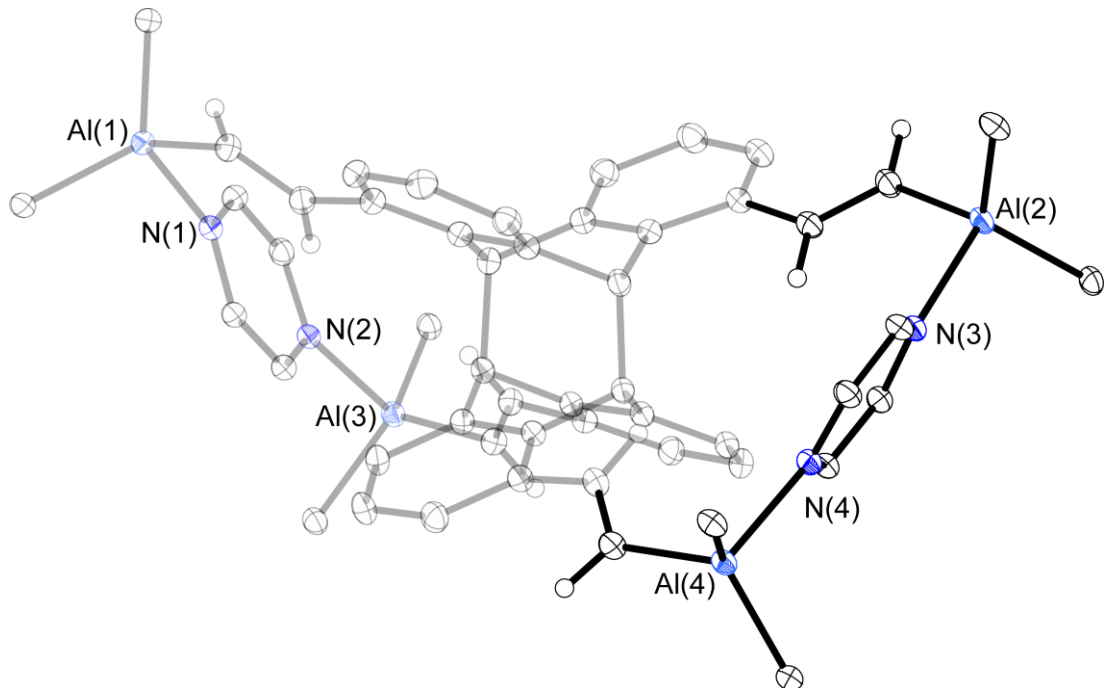


Figure S49a: Molecular structure of *anti*-9-PyZ₂ in the crystalline state from another point of view to highlight the diagonal binding of the pyrazine molecules. As in Fig 46 the displacement ellipsoids are drawn at the 40% probability level and H atoms (except vinylic hydrogen atoms which are greyed out) as well as SiMe₃ groups are omitted for clarity.

Table S1: Crystallographic data for compounds **A**, **3**, *anti*-**4**, *syn*-**5**, *anti*-**5** and *syn*-**6**.

	A	3 ^[a]	<i>anti</i> - 4	<i>syn</i> - 5 ^[b]	<i>anti</i> - 5	<i>syn</i> - 6 ^[c]
Empirical formula	C ₁₆ H ₈ O ₆ F ₆ S ₂	C ₂₄ H ₂₂ O ₂	C ₄₈ H ₅₂ Si ₄	C ₃₆ H ₂₀	C ₃₆ H ₂₀	C ₄₈ H ₄₄ O ₄ ·C ₃ H ₇ O
M _r	474.361	342.41	741.25	452.52	452.52	757.92
λ [Å]	0.71073	1.54184	1.54184	1.54184	1.54184	1.54184
T [K]	100.0(1)	100.0(1)	100.0(1)	100.0(1)	100.0(1)	100.0(1)
F(000)	238.4	364	1548	472	472	404
Crystal system	triclinic	triclinic	orthorhombic	monoclinic	monoclinic	triclinic
Space group	P $\bar{1}$	P $\bar{1}$	Pccn	P2 ₁ /c	P2 ₁	P $\bar{1}$
a [Å]	5.8009(2)	9.2137(3)	11.6681(7)	10.1803(3)	7.97671(17)	9.8534(6)
b [Å]	8.5919(2)	10.7277(4)	21.2988(13)	10.4962(3)	15.5959(3)	10.8417(7)
c [Å]	9.7054(2)	11.1202(3)	18.9147(9)	11.2236(3)	10.1573(2)	11.1079(6)
α [°]	69.951(2)	91.128(3)	90	90	90	92.036(5)
β [°]	73.313(2)	106.294(3)	90	106.591(3)	105.596(2)	102.618(5)
γ [°]	76.994(2)	112.674(3)	90	90	90	114.109(12)
V [Å ³]	430.94(2)	963.26(6)	4700.6(5)	1149.36(6)	1217.08(5)	1146.54(12)
Z	1	2	4	2	2	1
ρ _{calcd.} [g cm ⁻³]	1.828	1.181	1.047	1.308	1.235	1.203
μ [mm ⁻¹]	0.408	0.577	1.381	0.565	0.534	0.603
θ _{max} [°]	36.92	76.40	72.66	76.40	76.56	76.47
Index ranges <i>h</i>	-9 ≤ <i>h</i> ≤ 9	-11 ≤ <i>h</i> ≤ 10	-13 ≤ <i>h</i> ≤ 14	-12 ≤ <i>h</i> ≤ 12	-10 ≤ <i>h</i> ≤ 10	-10 ≤ <i>h</i> ≤ 12
Index ranges <i>k</i>	-14 ≤ <i>k</i> ≤ 14	-13 ≤ <i>k</i> ≤ 13	-26 ≤ <i>k</i> ≤ 26	-13 ≤ <i>k</i> ≤ 12	-19 ≤ <i>k</i> ≤ 19	-13 ≤ <i>k</i> ≤ 7
Index ranges <i>l</i>	-16 ≤ <i>l</i> ≤ 16	-13 ≤ <i>l</i> ≤ 13	-23 ≤ <i>l</i> ≤ 19	-13 ≤ <i>l</i> ≤ 14	-12 ≤ <i>l</i> ≤ 12	-13 ≤ <i>l</i> ≤ 13
Reflexes collected	40075	17949	10734	18751	21149	12900
Independent reflexes	4198	3951	4460	2395	4977	8016
R _{int}	0.0351	0.0222	0.0508	0.0324	0.0254	0.0391
Observed reflexes, <i>I</i> >2σ (<i>I</i>)	3936	3196	3351	2111	4805	5607
Parameters	172	484	241	203	326	365
R ₁ , <i>I</i> >2σ(<i>I</i>)	0.0217	0.0388	0.0738	0.0383	0.0317	0.0552
wR ₂ , <i>I</i> >2σ(<i>I</i>)	0.0528	0.1054	0.2043	0.0974	0.0832	0.1444
R ₁ (all data)	0.0237	0.0482	0.0931	0.0436	0.0331	0.0744
wR ₂ (all data)	0.0539	0.1112	0.2273	0.1022	0.0847	0.1530
GoF	1.175	1.049	1.043	1.042	1.035	0.937
ρ _{max} /ρ _{min} [e Å ⁻³]	0.44/-0.39	0.20/-0.23	0.97/-0.48	0.25/-0.20	0.17/-0.17 0.1(5)	0.36/-0.27
Flack parameter						
CCDC number	2163879	2163880	2163881	2163882	2163883	2163884

[a] Crystal was non-merohedrally twinned, component 2 rotated by 5.1° around [0.40 -0.91 -0.06] (reciprocal) or [0.16 -0.99 -0.04] (direct). One molecule is disordered at a centre of inversion. Hydrogen atoms were refined isotropically. [b] Hydrogens were refined isotropically. [c] Twinned crystal, ratio 64:36. Component 2 rotated by 2.5° around [0.39 0.77 -0.50] (reciprocal) or [0.63 0.76 -0.18] (direct). H1 and H2 were refined isotropically. Disorder of DMF over two sites near a centre of inversion (0.34:0.16).

Table S2: Crystallographic data for compounds **7**, **8**, *syn*-**9**, *anti*-**9**, *anti*-**9**·Py₄ and *anti*-**9**·Pyz₂.

	7 ^[a]	8 ^[a]	<i>syn</i> - 9	<i>anti</i> - 9 ^[b]	<i>anti</i> - 9 ·Py ₄ ^[c]	<i>anti</i> - 9 ·Pyz ₂
Empirical formula	C ₅₂ H ₁₀₄ Al ₂ Si ₁₀	C ₄₆ H ₈₈ Al ₂ Si ₈	C ₉₂ H ₁₇₆ Al ₄ Si ₁₆ ·2C ₆ H ₆	C ₉₂ H ₁₇₆ Al ₄ Si ₁₆ ·C ₆ H ₆	C ₁₁₂ H ₁₉₆ Al ₄ Si ₁₆ N ₄ ·2.5C ₆ H ₆	C ₁₀₀ H ₁₈₄ Al ₄ N ₄ Si ₁₆ ·10C ₆ H ₆
M _r	1064.21	919.84	1995.89	1917.79	2351.35	2780.94
λ [Å]	1.54184	1.54184	1.54184	1.54184	1.54184	0.71073
T [K]	100.0(1)	100.0(1)	100.0(1)	100.0(1)	100.1(1)	100.0(1)
F(000)	2328	1004	1088	2092	5108	3016
Crystal system	monoclinic	monoclinic	triclinic	triclinic	monoclinic	triclinic
Space group	<i>I</i> 2/ <i>a</i>	<i>P</i> 2 ₁ / <i>n</i>	<i>P</i> 1̄	<i>P</i> 1̄	<i>P</i> 2 ₁ / <i>c</i>	<i>P</i> 1̄
<i>a</i> [Å]	17.90519(19)	11.66217(18)	9.4442(12)	15.1482(3)	30.0412(3)	15.7845(3)
<i>b</i> [Å]	10.80972(12)	15.35916(16)	16.6757(15)	18.5350(3)	20.1721(1)	22.9127(5)
<i>c</i> [Å]	35.6601(5)	17.2597(2)	20.7613(16)	23.3981(4)	25.6654(3)	26.7425(5)
α [°]	90	90	99.270(7)	102.967(2)	90	111.110(2)
β [°]	98.7252(12)	106.3712(15)	96.849(8)	103.576(2)	108.0983(3)	103.729(2)
γ [°]	90	90	99.523(9)	97.456(2)	90	96.176(2)
<i>V</i> [Å ³]	6822.13(14)	2966.23(7)	3146.5(6)	6106.6(2)	14783.6(3)	8563.8(3)
<i>Z</i>	4	2	1	2	4	2
ρ _{calcd.} [g cm ⁻³]	1.036	1.030	1.053	1.043	1.056	1.078
μ [mm ⁻¹]	2.280	2.184	2.094	2.140	1.857	0.186
θ _{max} [°]	76.52	76.47	68.08	77.02	76.59	32.32
Index ranges <i>h</i>	-22 ≥ <i>h</i> ≥ 19	-14 ≥ <i>h</i> ≥ 13	-11 ≥ <i>h</i> ≥ 10	-19 ≥ <i>h</i> ≥ 19	-37 ≥ <i>h</i> ≥ 37	-23 ≥ <i>h</i> ≥ 23
Index ranges <i>k</i>	-13 ≥ <i>k</i> ≥ 13	-19 ≥ <i>k</i> ≥ 19	-11 ≥ <i>k</i> ≥ 19	-23 ≥ <i>k</i> ≥ 23	-25 ≥ <i>k</i> ≥ 25	-32 ≥ <i>k</i> ≥ 33
Index ranges <i>l</i>	-44 ≥ <i>l</i> ≥ 44	-21 ≥ <i>l</i> ≥ 21	-24 ≥ <i>l</i> ≥ 24	-27 ≥ <i>l</i> ≥ 29	-25 ≥ <i>l</i> ≥ 31	-40 ≥ <i>l</i> ≥ 38
Reflexes collected	34270	47794	25547	124476	294394	179787
Independent reflexes	7067	6160	11176	25339	30812	55632
R _{int}	0.0298	0.0889	0.1554	0.0573	0.0841	0.0443
Observed reflexes, <i>I</i> >2σ (<i>I</i>)	6278	5407	4877	20284	23393	40002
Parameters	497	429	584	1142	1273	1705
R ₁ , <i>I</i> >2σ(<i>I</i>)	0.0310	0.0371	0.1001	0.0538	0.0574	0.0632
wR ₂ , <i>I</i> >2σ(<i>I</i>)	0.0808	0.0974	0.2396	0.1331	0.1518	0.1698
R ₁ (all data)	0.0360	0.0428	0.1813	0.0687	0.0758	0.0920
wR ₂ (all data)	0.0847	0.1022	0.3201	0.1455	0.1653	0.1856
GoF	1.038	1.030	0.969	1.044	1.037	1.075
ρ _{max} /ρ _{min} [e Å ⁻³]	0.36/-0.28	0.52/-0.35	0.65/-0.61	0.86/-0.95	0.99/-0.55	0.70/-0.40
CCDC number	2163885	2163886	2163887	2163888	2163889	2180919

[a] All hydrogen atoms were refined isotropically. [b] One SiMe₃- group is disordered with ratio 56:44, SIMU restraints were applied for disordered atoms. [c] Crystal contains 2.5 benzene molecules per asymmetric unit, which could not be refined reasonably, therefore, a solvent mask was calculated and 408 electrons were found in a volume of 2956 Å³ in 3 voids per unit cell. This is consistent with the presence of 2.5 benzene molecules per formula unit which account for 420 electrons per unit cell.

References

1. O. V. Dolomanov, L. J. Bourhis, R. J. Gildea, J. A. K. Howard and H. Puschmann, *J. Appl. Cryst.* 2009, **42**, 339–341.
2. (a) G. M. Sheldrick, *Acta Crystallogr., Sect. A* 2008, **64**, 112–122, (b) G. M. Sheldrick, *Acta Crystallogr., Sect. A* 2015, **71**, 3–8.
3. G. M. Sheldrick, *Acta Crystallogr., Sect. C* 2015, **71**, 3–8.
4. F. Kleemiss, O. V. Dolomanov, M. Bodensteiner, N. Peyerimhoff, L. Midgley, L. J. Bourhis, A. Genoni, L. A. Malaspina, D. Jayatilaka, J. L. Spencer, F. White, B. Grundkötter-Stock, S. Steinhauer, D. Lentz, H. Puschmann and S. Grabowsky, *Chem. Sci.*, 2021, **12**, 1675–1692